Nanoparticles in Liquid Crystals: Synthesis, Self-Assembly, Defect Formation and Potential Applications

Article *in* Journal of Inorganic and Organometallic Polymers and Materials · June 2007

DOI: 10.1007/s10904-007-9140-5

3 authors, including:

Torsten Hegmann
Kent State University
99 PUBLICATIONS **1,971** CITATIONS
SEE PROFILE

Vanessa Marx
California Institute of Technology
35 PUBLICATIONS **795** CITATIONS
SEE PROFILE

Journal of Inorganic and Organometallic Polymers and Materials, Vol. 17, No. 3, September 2007 (© 2007)
DOI: 10.1007/s10904-007-9140-5

Review

Nanoparticles in Liquid Crystals: Synthesis, Self-Assembly, Defect Formation and Potential Applications

Torsten Hegmann,[1,*] Hao Qi,[1] and Vanessa M. Marx[1]

Accepted December 5, 2006

Torsten Hegmann is an Assistant Professor of Chemistry at the University of Manitoba in Winnipeg, Manitoba. He received his M.Sc. (diploma) and Ph.D. (Dr. rer. nat.) at the Martin-Luther University Halle-Wittenberg (Germany) in Prof. Carsten Tschierske's group working on macrocyclic liquid crystals and metallomesogens, and carried out postdoctoral work as a DAAD/NATO fellow with Prof. Robert P. Lemieux at Queen's University in Kingston, Ontario investigating chirality transfer mechanisms in ferroelectric liquid crystal mixtures. In 2003, he joined the Department of Chemistry at the University of Manitoba. His primary research interests are the synthesis and characterization of liquid crystals and nanomaterials, and structure-property relationships as well as self-assembly processes in liquid crystals and liquid crystal nanocomposites. In 2006, he received an Ichikizaki Award from the Canadian Society for Chemistry.

Hao Qi completed his B.E. degree at Sichuan University, and his M.Sc. in Applied Chemistry at the Research Institute of Petroleum Processing of China in 2003 under the supervision of Prof. Danping Wei working on nanostructured clays as lubricant systems. In 2004, he started his Ph.D. thesis in Dr. Hegmann's group. His work is focused on the synthesis of functionalized metal nanoparticles and liquid crystals as well as on the fabrication of ordered liquid crystal nanocomposites.

[1] Department of Chemistry, University of Manitoba, 144 Dysart Road, R3T 2N2, Winnipeg, MB, Canada.
* To whom correspondence should be addressed.
E-mail: hegmannt@cc.umanitoba.ca

Vanessa M. Marx is currently completing her undergraduate degree (Hons.) at the University of Manitoba. She joined Dr. Hegmann's group as an NSERC summer research student in 2006, and is currently working as a research project student investigating liquid crystal functionalized gold nanoparticles using mesogenic groups with unusual molecular shape.

ABSTRACT Revolutionary developments in the fabrication of nanosized particles have created enormous expectations in the last few years for the use of such materials in areas such as medical diagnostics and drug-delivery, and in high-tech devices. By its very nature, nanotechnology is of immense academic and industrial interest as it involves the creation and exploitation of materials with structural features in between those of atoms and bulk materials, with at least one dimension limited to between 1 and 100 nm. Most importantly, the properties of materials with nanometric dimensions are, in most instances, significantly different from those of atoms or bulk materials. Research efforts geared towards new synthetic procedures for shape and size-uniform nanoscale building blocks as well as efficient self-assembly protocols for manipulation of these building blocks into functional materials has created enormous excitement in the field of liquid crystal research. Liquid crystals (LCs) by their very nature are suitable candidates for matrix-guided synthesis and self-assembly of nanoscale materials, since the liquid crystalline state combines order and mobility at the molecular (nanoscale) level. Based on selected relevant examples, this review attempts to give a short overview of current research efforts in LC-nanoscience. The areas addressed in this review include the synthesis of nanomaterials using LCs as templates, the design of LC nanomaterials, self-assembly of nanomaterials using LC phases, defect formation in LC-nanoparticle suspensions, and potential applications. Despite the seeming diversity of these research topics, this review will make an effort to establish logical links between these different research areas.

KEY WORDS: defects; liquid crystal; liquid crystals; nanochemistry; nanoclusters; nanomaterials; nanoparticles; self-assembly; self-organization; template synthesis

1. INTRODUCTION

In recent years, revolutionary developments in the fabrication of nanomaterials have created enormous expectations for the application of such materials in high-tech and medical devices. By its very nature, nanotechnology is of immense academic and industrial interest as it involves the creation and exploitation of materials with structural features between those of atoms and bulk materials with at least one dimension limited to between 1 and 100 nm [1–3]. Viewed as the driving force for nanotechnology research, the properties of materials with nanometric dimensions significantly differ from those of atoms or bulk materials. Suitable control of the properties of nanometer-scale structures will enable new science as well as new products, devices, and technologies. One of the central challenges of nanotechnology today is to discover new methods for reliably assembling nanoscale building blocks into functional bulk materials. A focus of current research worldwide is to design nanomaterials that are able to self-assemble into larger, organized structures [4–6].

Liquid crystalline materials appear as perfect candidates for the synthesis and self-assembly of nanoscale materials as the liquid crystalline state combines order and mobility at the molecular, nanoscale level. Composed of anisotropic molecules, liquid crystals respond to external fields and interact with surfaces, thus influencing their structure and properties [7]. Liquid crystals have gained acceptance in many scientific communities. The concepts of orientational order and collective molecular motion are recognized in bioscience, serving as model systems for cell membranes and muscles. In addition, liquid crystals have found widespread use in information displays, as sensors, drug delivery vehicles, in flexible displays, in photonic band gap structures, as well as in optical elements such as controllable lenses and lasing [8, 9]. Liquid crystal science and technology is crossing the boundaries of many fundamental scientific disciplines, and has already made very important contributions to nanoscience and nanotechnology.

At first, to familiarize the reader with the liquid crystalline state, we start with a crude classification of liquid crystal materials into solvent-dependent and

solvent-less liquid crystal phase with some emphasis on the driving forces for liquid crystal phase formation such as self-assembly (self-organization), attractive interactions and micro-segregation of incompatible molecular segments [7].

For many materials (pure compounds or mixtures) liquid crystalline phases (also termed mesophases) are observed in a multi-step process at the transition from the highly ordered crystalline state with long range orientational and positional ordering to the disordered liquid state (or *vice versa*) *via* the formation of one or more intermediate phases. In these phases, the order of the crystalline state is partially lost, and the constituent molecules, aggregates, or particles possess some degree of mobility (i.e. translational, rotational, and/or conformational freedom) [10]. These liquid crystalline (LC) phases can occur in pure materials or mixtures in the absence of a solvent depending solely on the temperature (thermotropic LC phases) [11–13] or in multi-component systems in the presence of a solvent depending on the temperature and the composition (lyotropic LC phases).

Traditionally, substances or materials capable of forming LC phases (mesogens) were divided into two classical categories: (i) non-amphiphilic anisometric mesogens most commonly displaying exclusively thermotropic LC phases, and (ii) amphiphilic mesogens which usually show lyotropic LC phases [12, 14]. A third category termed amphotropic LCs would cover all those LC materials capable of forming both lyotropic as well as thermotropic LC phases (Fig. 1) [11]. Both anisometric and amphiphilic mesogens have been successfully integrated into main-chain and side-chain LC polymers [15–17], attached to (or incorporated into) dendritic cores [18, 19], or were amalgamated in many unique ways by combining anisometric mesogenic units with amphiphilic moieties contributing to an increasingly diminishing boundary between lyotropic and thermotropic LC behaviour [11, 13, 20]. For both types, regardless of the molecular shape and structure of the constituent entities, LC phases can be classified using elements of symmetry and the degree of long-range ordering. Although quite a number of LC phases exist that are unique to each of the classical types of lyotropic and thermotropic LC materials (as can be seen in Figs. 2 and 3), it seems useful to introduce them together depending on the degree of positional and orientational ordering [21], molecular shape, or interface curvature. Whereas mesophase formation in lyotropic liquid crystals is driven by the segregation of

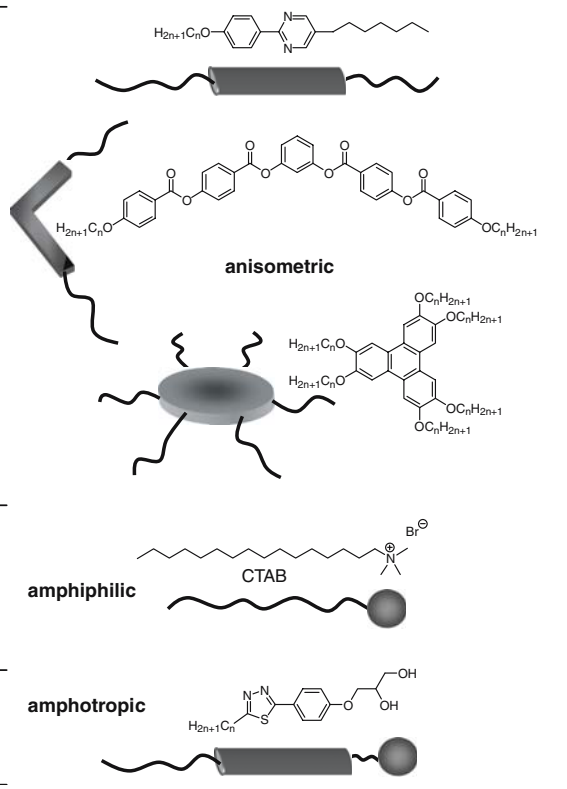

Fig. 1. Typical examples (and molecular shapes) of the main types of molecules forming LC phases.

hydrophobic or hydrophilic regions (hydrophobic effect) of an amphiphilic molecule from a solvent, mesophase formation in thermotropic liquid crystals is driven by the segregation of chemically incompatible subunits from one another, such as the segregation of rigid aromatic cores from flexible alkyl tails within a molecule.

In the nematic phase, the least ordered LC phase, the constituents solely possess orientational ordering and no positional ordering. As can be seen in Fig. 2, unidirectional alignment of the molecules results in a purely orientational ordered structure [11]. The nematic phase generally results when the volume fraction of an incompatible core unit far exceeds that of the incompatible wings, and may result for both rod- and disk-shaped molecules. In this phase the molecules, aggregates, or particles are aligned (on the time-average) along a common direction, also termed the director *n*. The director is oriented either parallel to the long molecular axis for rod-like molecules or particles (N, uniaxial nematic phase), parallel to the column axis for columnar aggregates formed by amphiphilic (i.e. rod-like micelles) or disk-like molecules (N_{Col}, columnar

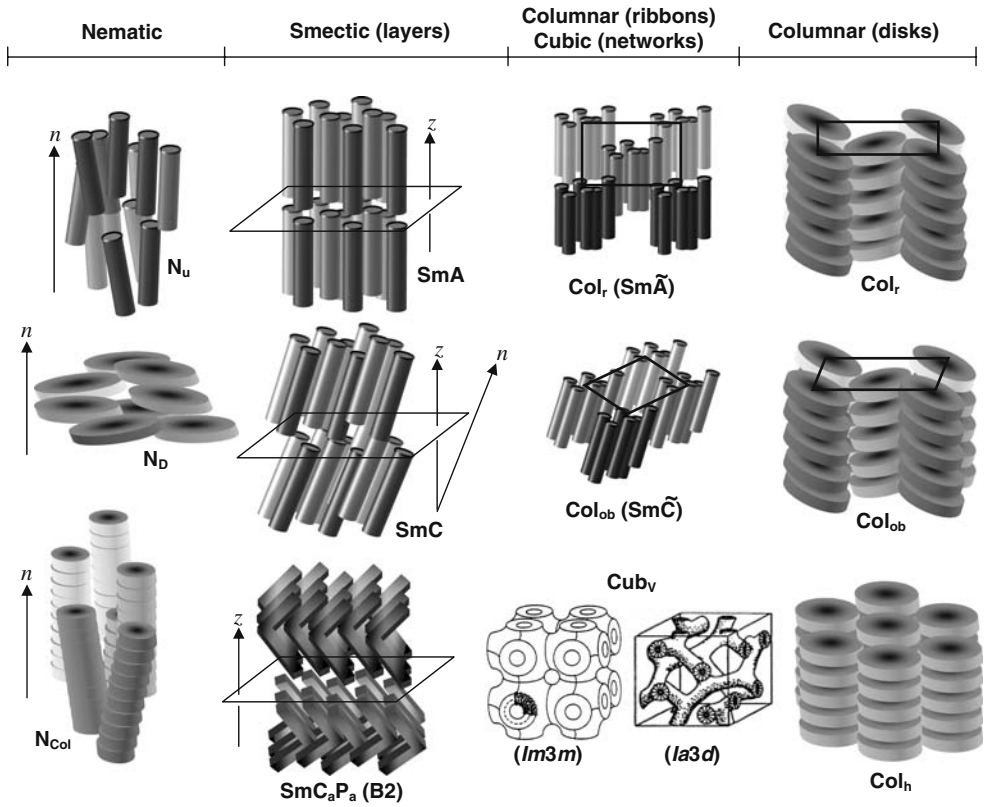

Fig. 2. Presentation of the main types of nematic and positional ordered thermotropic LC phases formed by rod-like, disk-like, polycatenar and amphiphilic molecules. Abbreviations: N_u = uniaxial nematic phase, N_D = discotic nematic phase, N_{Col} = columnar nematic phase, L_α = lamellar or smectic-A phase, SmA = smectic-A phase, SmC = smectic-C phase, SmC_aP_a = anticlinic antiferroelectric polar smectic-C phase, Col_r = rectangular columnar phase, Col_{ob} = oblique columnar phase, Col_h = hexagonal columnar phase, Cub_V = bicontinuous cubic phase, Cub_I = micellar cubic phase (space groups are in italics).

nematic phase), or parallel to the short molecular axis for disk-like aggregates of amphiphiles (i.e. plate-like micelles), molecules, or particles (N_D, discotic nematic phase) [22]. The chiral version of the nematic phase, the chiral nematic or cholesteric phase (N* – the asterisk indicating chirality of the phase) is characterized by a continuous helical distortion (helical twist) of the director *n* along the long molecular axis. Because of its response to applied electric fields and surfaces, the N* phase is used in a variety of technological applications such as flat panel liquid crystal displays (LCDs, e.g. twisted nematic and super-twisted nematic displays) and temperature sensing, using an effect called selective reflection of light that is operational at wavelengths commensurate with the helical pitch of the N* phase [23].

The most prominent LC phases with positional ordering are smectic (Sm), columnar (Col), and cubic (Cub) phases. Elongated rod-like (calamitic) molecules or particles (also described as spherocylinders) commonly form smectic (or lamellar) phases with layer ordering. In the absence of additional positional ordering within the layers [24], the two most important smectic modifications [25] are the smectic-A phase (SmA), in which the long molecular axes of the molecules are (on the time average) aligned orthogonal to the layer planes, and the smectic-C phase (SmC), in which the molecules are tilted with respect to the layer normal [26]. The chiral versions of both phases (SmA*, SmC*) are formed by chiral mesogens or by doping the non-chiral phase with an appropriate chiral dopant, and are both widely used in electro-optic devices due to their unique response to applied electric fields (the electroclinic effect in the SmA* phase [27–30], and surface-stabilized ferroelectric switching in the SmC* phase [31–34]). Rod-like molecules (predominantly polycatenar molecules) have also been reported to form columnar phases (Col_r, Col_{ob}), in which the smectic layers collapse into ribbons that organize in a rectangular or an oblique 2-D lattice. These molecules may also form bicontin-

uous cubic phases with a different symmetry or space group (*Ia*3*d*, *Im*3*m*).

Another interesting group of chiral LC phases arises from frustration either of space filling in three dimensions with a double twist structure, which can not fill space completely, resulting in the formation of defects that stabilize the structure, or the competition between layer packing and the need of chiral molecules to form a helical structure due to chiral packing requirements. This group of LC phases, commonly referred to as "frustrated phases", includes the nematic-type blue phases (BPI, BPII, and BPIII or "fog" phase), smectic blue phases ($BP_{Sm}I$, and $BP_{Sm}II$), as well as twisted grain boundary phases (TGBA*, and TGBC*). Since a discussion of these complex frustrated phases is far out of the scope of this review, the reader is referred to a leading article by Goodby [35].

Discotic or disk-like molecules, as one would anticipate, prefer forming columnar phases in which the disk-like molecules, aggregates, or particles pack to form columns that can organize into arrays with a different symmetry such as hexagonal (Col_h), rectangular (Col_r), oblique (Col_{ob}), or tetragonal (Col_{tet}) [36, 37].

In addition to the aforementioned conventional mesogens (rod or disk-like), recent research efforts in the LC field have increasingly focused on so-called non-conventional LCs or mesogens that are neither purely rod nor disk-shaped. Such non-conventional mesogens can give rise to unique transitions between different phase morphologies, for example from a lamellar to a columnar molecular packing. Owing to their unusual shape, structure, and connectivity of incompatible molecular segments, micro-segregation of incompatible molecular subunits and space filling effects are commonly discussed as the main driving forces for LC phase formation. Beautifully reviewed by Tschierske [12] non-conventional LCs include, but are not limited to, cyclic and open-chain oligoamides [12], polyether macrocycles [38], several types of metallomesogens (metal-containing LCs) [39–41], low-aspect ratio LCs with tetrahedral [42] or octahedral cores [43], polyhydroxy and taper-shaped amphiphiles [44], laterally substituted calamitics [45], dendrimers [18], polyfluorinated LCs [46], oligosiloxanes [47], and bent-core (banana-shaped) LCs.

Bent-core LCs [48–50] in particular have received enormous attention over the past decade or so owing to the unique effects resulting from the sterically induced packing of the bent-core mesogens, such as the formation of helical (chiral) superstructures in the B7 phase [51], as well as the formation of chiral layer structures without the necessity of chiral mesogens such as the formation of a conglomerate in a fluid as observed for the first time by Clark and Walba *et al*. in polar smectic-C phases, SmCP [52] (B2 family with two conglomerates and two macroscopic racemates – as an example see the anticlinic antiferroelectric polar smectic-C phase, SmC_aP_a at the bottom of Fig. 2).

Amphiphilic molecules such as surfactants and lipids can form a wide variety of LC phases in the pure state [11] (thermotropic phases, see above). In addition, their mesomorphic properties can be influenced by the addition of solvents (protic and aprotic) leading to the formation of lyotropic LC phases [53]. For example, amphiphiles will form micellar structures in aqueous solution once a certain concentration, termed the critical micelle concentration (*cmc*), has been reached. The insoluble hydrophobic portions will segregate from the soluble hydrophilic portions. Both the molecular shape of the amphiphilic molecule and the amphiphile/water ratio will determine the packing geometry of the hydrophilic and hydrophobic portions of the molecule (interface curvature of the incompatible hydrophilic and hydrophobic counterparts of the amphiphile), and as a result will determine the type of the LLC phase that is formed (see Fig. 3) [14].

When the amphiphile/water ratio is low such as found to the right of Fig. 3, segregated micellar structures result forming micellar cubic structures (Cub_I). Increasing the amphiphile/water ratio results in the formation of hexagonal columnar phases (Col_h) and further to interwoven networks organized into different lattices (bicontinuous cubic phases, Cub_V). As the ratio further increases, curved interfaces are no longer formed and a layer structure results (lamellar phases, L_α or SmA). A continued increase in the amphiphile/water ratio will eventually result in the formation of reverse bicontinuous cubic as well as columnar phases, where the solvent itself segregates inside the hydrophilic regions of the amphiphile, up until the point where a reverse micellar cubic lattice is formed. In addition to the general type of LLC phase formed, the length and the number of the alkyl tails forming the hydrophobic component of the amphiphile will have a profound impact on the diameter of cylindrical aggregates (columnar and cubic phases), or the interlayer spacing in the case of the lamellar phase.

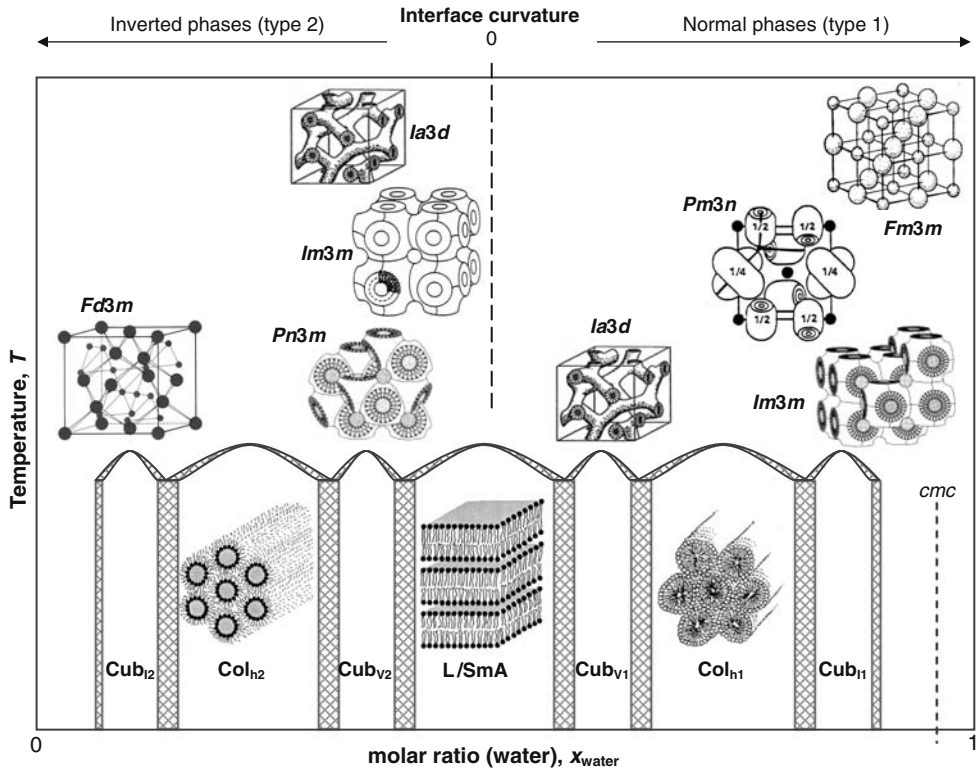

Fig. 3. Presentation of the main types of lyotropic LC phases depending on the interface curvature (molecular shape or concentration in water as the most commonly used solvent). * For abbreviations see caption Fig. 2.

2. SCOPE OF THIS REVIEW

In this review, we will highlight the particular role liquid crystalline materials play in the synthesis and preparation of size and shape-uniform nanostructures, the use of condensed liquid crystal phases for nanoparticle assembly, and on interactions between nanomaterials and liquid crystal phases leading to unique defect structures or to new and exciting properties for the use of this materials combination in high-tech applications.

3. SYNTHESIS USING LCS AND LC TEMPLATES

As the properties of nanoscale materials are size- and shape-dependent [54–58], a prerequisite for the development of functional nanomaterial arrays are nanobuilding blocks of uniform size and shape. Liquid crystals combine both order and mobility on the molecular (*nanoscale*) level, and as such, liquid crystal phases are ideal candidates for controlled nanoparticle synthesis.

In this section, we address the evolution of nanoparticle synthesis (nanorods in particular) using liquid crystal molecules, commencing with lyotropic liquid crystals fulfilling the simple role of surfactants and phase transfer agents, and evolving from their use as pure templating agents to ''nanoreactors'' [59] where nanoparticles assemble within the liquid crystalline phase itself. We will also point out the use of thermotropic liquid crystals in the synthesis of polymeric as well as metal nanostructures.

3.1. Lyotropic LCs as surfactants and phase transfer agents

A notable concern in nanoparticle synthesis is the ability to prepare air- and thermally-stable particles of controlled size and dispersity, which may also be repeatedly isolated and re-dissolved in organic solvents without irreversible aggregation and decomposition [60].

The Brust–Schiffrin method for the synthesis of monolayer-protected clusters [61–69] exploits surfactant molecules such as tetraoctylammonium bromide

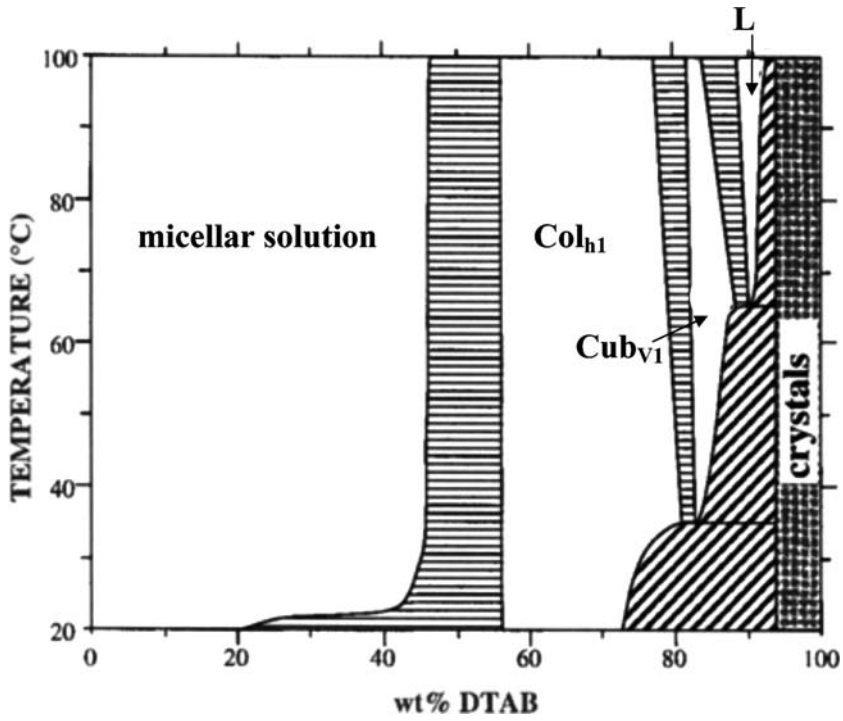

Fig. 4. Partial phase diagram of the binary DTAB/water system: Col_{h1}, normal hexagonal phase; Cub_{V1}, bicontinuous cubic phase (*Ia3d*); L_{α}, lamellar phase; crystals, hydrated DTAB crystals. The horizontally shaded areas (showing tie lines) indicate a region where two liquid crystalline phases coexist and the diagonally shaded areas indicate coexistence between a liquid crystalline phase and hydrated crystals. Reprinted with permission from K. M. McGrath, *Langmuir* **11**, 1835 (1995), [77]. Copyright 1995 American Chemical Society.

(TOAB, which is not capable of forming lyotropic LC phases) as phase transfer agents.

While the Brust–Schiffrin reaction is generally confined to the production of spherical nanoparticles, shape-control may also be achieved through changing the reducing agent, the stabilizer concentration, and/or the structure of the surfactant [70–72]. Murphy and Jana have successfully synthesized gold [54] and silver [73] nanorods through a seed-mediated growth approach. In this approach, spherical nanoparticles with a diameter of 3.5 ± 0.7 nm (''seeds'') are initially produced through hydride reduction of hydrogen tetrachloroaurate [54] or silver nitrate [73] in the presence of sodium citrate. These nanoparticles are then transferred to a solution containing cetyltrimethylammonium bromide (CTAB), and additional hydrogen tetrachloroaurate or silver nitrate. The resultant rod-shaped particles are collected following centrifugation [54, 73].

It was later discovered that addition of sodium hydroxide along with CTAB and ascorbic acid in the second step results in longer (higher aspect ratio) nanorods [54], and that this approach also works in combination with nanoporous membrane-based techniques avoiding the formation of other nanoparticle shapes [74]. This particular synthetic pathway favours rod formation for two reasons. First, CTAB acts as a directing agent by forming a bilayer on the gold nanorods. CTAB binds stronger to the side edges than the ends of the nanorods and thus only allows growth in one direction. In this way CTAB (an ionic amphiphile capable of forming a variety of LLC phases [75, 76] – see analogue phase diagram of DTAB in Fig. 4 [77]) plays a critical role in the formation of 1-D nanostructures (Fig. 5). Secondly, ascorbic acid is a weak reducing agent incapable of reducing hydrogen tetrachloroaurate in the absence of the gold seeds, and hence minimal additional nucleation occurs during particle growth [54].

Additional examples for LLC surfactant-assisted growth of nanorods have been successfully demonstrated for tellurium nanorods [78] and selenium nanowires [79].

3.2. True liquid crystal templating

Considering the structural diversity of LCC phases (in particular the hexagonal columnar phases

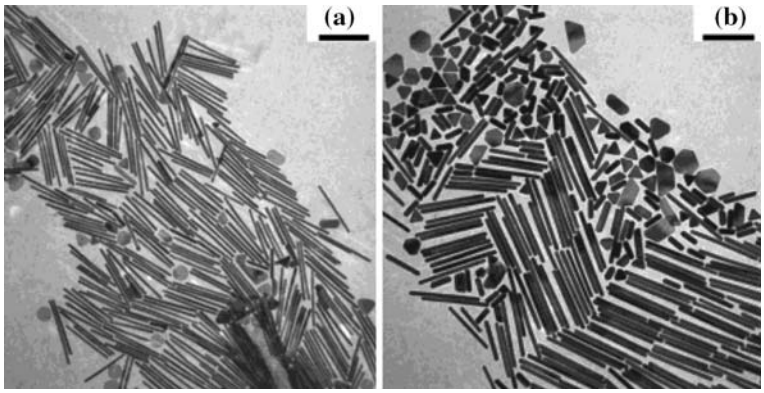

Fig. 5. TEM micrographs of gold nanorods synthesized from: (a) CTAB-stabilized 8 nm seeds and, (b) CTAB-stabilized 16 nm seeds (scale bars measure 500 nm). Reprinted with permission from A. Gole, and C. J. Murphy, *Chem. Mater*. **16**, 3633 (2004), [73b]. Copyright 2004 American Chemical Society.

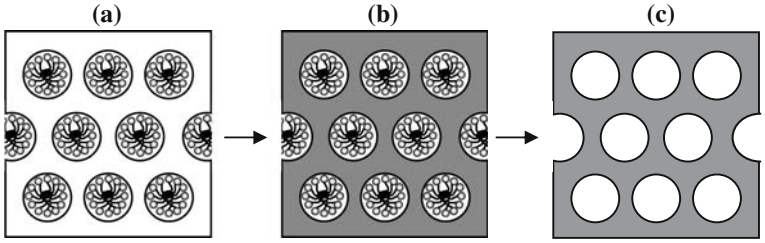

Fig. 6. Schematic representation of the 'nanocasting': (a) ordered parent LLC phase, (b) addition of liquid continuous phase, and (c) calcination of parent LLC phase resulting in an ordered porous material. Adapted from S. Polarz and M. Antonietti, *Chem. Commun*. 2593 (2002), [82].

in Fig. 3), it is easy to imagine how LLC phases may be used as templates for the synthesis of mesoporous nanostructures, which result in porous inorganic replicates of the parent LLC upon calcination [80, 81]. This procedure allows for the production of materials with uniform pore size, morphology, and 3-D distribution in addition to obtaining control over their properties and macroscopic shape. An additional advantage of LLC templating is that pore sizes may be increased through addition of a hydrophobic component due to expansion of the interior of the micelle. Hence, this technique is an application of what is termed 'true liquid crystal templating' or 'nanocasting' [80], and is currently widely used in the synthesis of porous media used in applications for catalysis or adsorption techniques (see Fig. 6) [82–84].

The liquid continuous phase shown in Fig. 6b may either be composed of a siliceous material or an aqueous metal salt. In the latter case, reduction of the metal salt results in the formation of an ordered network of nanoparticles surrounding the micelles of the liquid crystalline host, and upon calcination a porous nanostructure is obtained retaining the structure of the original LLC. Hence, LLC templating is restricted to the formation of frameworks that will remain stable upon surfactant removal and exposure to air/water [85, 86].

Many types of silica-based [87–92] (Fig. 7a) as well as non-siliceous mesoporous nanomaterials have been successfully synthesized through LLC templating using polymer or oligomer surfactant systems. Examples of non-siliceous mesoporous structures consist of numerous metal oxides [87, 93], CdS and CdSe composites [94], Pt/Ru alloys, and Ni/Co alloys [95]. Several additional examples have been reported for platinum, cobalt [96], palladium [97] (Fig. 7b), nickel [98] (Fig. 7c), rhodium [99], selenium [100], tellurium [101], tin [102], copper [103], as well as cadmium [103].

3.3. Reverse templating

The LLC phase itself may be used to generate an ordered array of nanoparticles synthesized within the hydrophobic regions of reverse micelles (or hydrophilic regions of normal micelles). In this case, the LLC acts as a nanosupport or 'nanoreactor', and

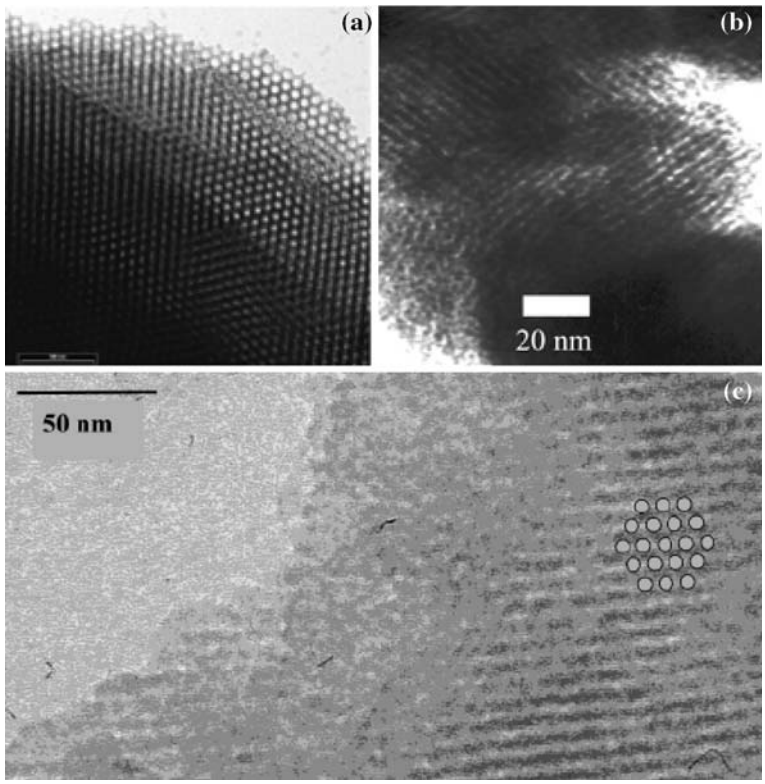

Fig. 7. Transmission electron micrograph of: (a) calcined silica nanocast obtained by using poly(ethylene-*co*-butylene)-*block*-poly(ethylene oxide) (KLE-2) as template (scale bar is 100 nm). Reprinted with permission from A. Thomas, H. Schlaad, B. Smarsly, and M. Antonietti, *Langmuir***19**, 4455 (2003), [91]. Copyright 2003 American Chemical Society. (b) nanostructured Pd deposited by electrochemical reduction of palladium ions dissolved in the aqueous domains of a hexagonal columnar lyotropic liquid crystalline phase (H_1-e Pd) using $C_{16}EO_8$ (octaethyleneglycol monohexadecyl ether). From P. N. Bartlett, B. Gollas, S. Guerin, and J. Marwan, *Phys. Chem. Chem. Phys.* **4**, 3835 (2002), [97]. Reproduced with permission from the PCCP Owner Societies. (b) Brij56-templated Ni showing the ordered mesoporosity of the hexagonal columnar (Col_{h1}) structure. Ni was electrodeposited at 25 °C and -900 mV *vs.* SCE. (The overlaid hexagonal pattern shows the structure of the template.) Reprinted with permission from P. A. Nelson, J. M. Elliot, G. S. Attard, and J. R. Owen, *Chem. Mater.* **14**, 524 (2002), [98]. Copyright 2002 American Chemical Society.

hence by controlling the type of liquid crystalline phase one may control the size and shape of the nanoparticles grown within [104, 105]. An additional advantage is that the preparation of these 'nanoreactors' is easily reproducible, and can be generated in large volume [106].

LLCs such as surfactant/water systems forming lamellar or hexagonal columnar morphologies were selected to prepare metallic NPs [107–109] or nanostructured conducting polymers [110].

In a typical metal nanoparticle synthesis, a solution of the metal salt is mixed with an appropriate amount of the liquid crystalline host such that the desired LLC phase is formed. Precipitation of the nanoparticles is induced, which aggregate into clusters that subsequently form a single nanostructure. As this nanostructure will typically take on the shape of the original nano-domain, columnar phases typically form rod-like nanostructures whereas cubic and lamellar phases usually result in spherical or disc-like nanostructures (see Fig. 8) [104, 111]. Following dispersion of the LLC phase, the resulting nanostructures are then collected through centrifugation or filtering.

Dellinger and Braun have demonstrated the utility of using LLCs as nanoreactors for the synthesis of nanosized BiOCl [106]. Here, both a lamellar and a hexagonal columnar LC host were used. The host LLC was added to aqueous $BiCl_3$ while simultaneously heating and stirring, and upon cooling to room temperature BiOCl was precipitated through the diffusion of ammonia into the LLC lattice. It was discovered that the lamellar LLC phase produced roughly spherical 5.0 nm particles. Meanwhile, the hexagonal LLC phase produced monodisperse arrow-shaped rods 100 nm wide and 250 nm long. This is comparable to particles synthesized in an isotropic fluid as a control experiment, where a series

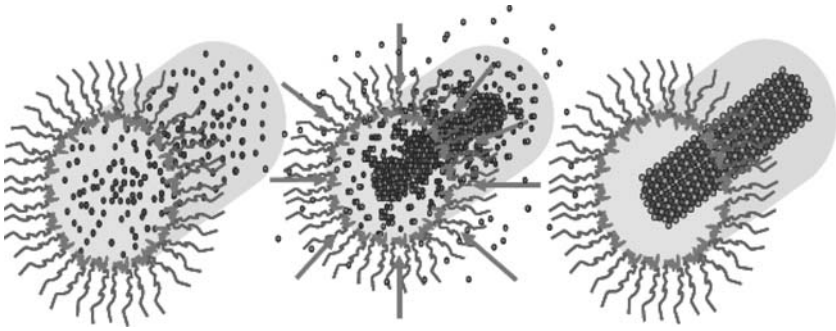

Fig. 8. Schematic representation of nanoparticle synthesis utilizing LLCs as nanoreactors. Reprinted from G. N. Karanikolos, P. Alexandridis, R. Mallory, A. Petrou, and T. J. Mountziaris, *Nanotechnology* **16**, 2372 (2005), [111] with permission from IOP Publishing Ltd.

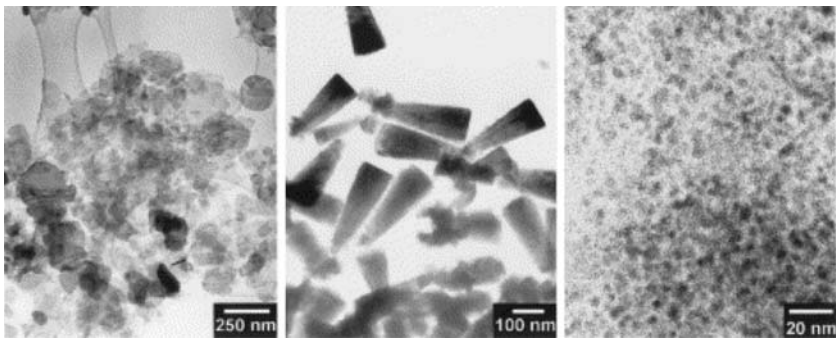

Fig. 9. TEM micrographs of BiOCl produced (a) in free solution, (b) in the hexagonal liquid crystal, and (c) in the lamellar liquid crystal. Reprinted from T. M. Dellinger and P. V. Braun, *Scripta Mater*. **44**, 1893 (2001), [106] with permission from Elsevier.

of disks ranging from 50 to 250 nm in diameter were produced (Fig. 9) [106].

Mountziaris *et al*. have successfully synthesized ZnSe nanowires, nanodisks, and quantum dots [111, 112]. In this case, a solution of the host LLC in formamide is mixed with a solution of heptane containing diethylzinc, and H_2Se is allowed to diffuse into the LLC-diethylzinc matrix. Upon diffusion into the hexane-diethylzinc nanodomains, ZnSe particles are formed. A hexagonal LLC phase was used to form the nanowires (average diameter 3.0 nm), and a lamellar phase was used to form nanodisks with an average thickness of 6.0 nm. A cubic LLC phase allowed for the production of spherical quantum dots with an average diameter of 3.0 nm, whose photoluminescence spectrum was noted to be blue-shifted by $\sim$30 nm in comparison to the bulk material (Fig. 10) [111].

Carpenter *et al*. have exploited the controlled environment available within the reverse micelles of an LLC phase for the synthesis of ferrite (Fe_3O_4) nanoparticles coated with MnO [113].

A variety of nanostructures have been successfully synthesized using a LLC matrix. Examples of nanowires include those of silver [55, 114–117], ZnS [118, 119], Cu [120], $CaSO_4$ [121] $BaCO_3$ [122], and $BaSO_4$ [123] Spherical nanoparticles of Bi [108], Pd [104], PbS [124], $KMnF_3$ [125], $BaSO_4$ [121], γ-Fe_2O_3, Fe_3O_4, $MnFe_2O_4$, and $CoFe_2O_4$ [113] have also been reported, as well as an example of spherical iron nanoparticles encapsulated within a thin gold film [126].

3.4. Thermotropic LC phases in nanoparticle synthesis

As outlined in the introduction, thermotropic LCs, which self-assemble into ordered structures similar to those seen for LLC mesophases without the prerequisite of solvent addition, have many additional possibilities not present for the lyotropic phase such as tilted smectic phases (SmC), biaxial or polar smectic-A phases [127], and non-hexagonal columnar (e.g., Col_r) phases [12].

Guymon *et al*. have made interesting use of the condensed smectic phase for the synthesis of polymeric nanostructures of fluorinated acrylates [128, 129]. This procedure involves mixing the monomer with the host thermotropic LC, and polymerization is initiated at a suitable temperature where the host LC displays liquid crystalline order [130]. It has been

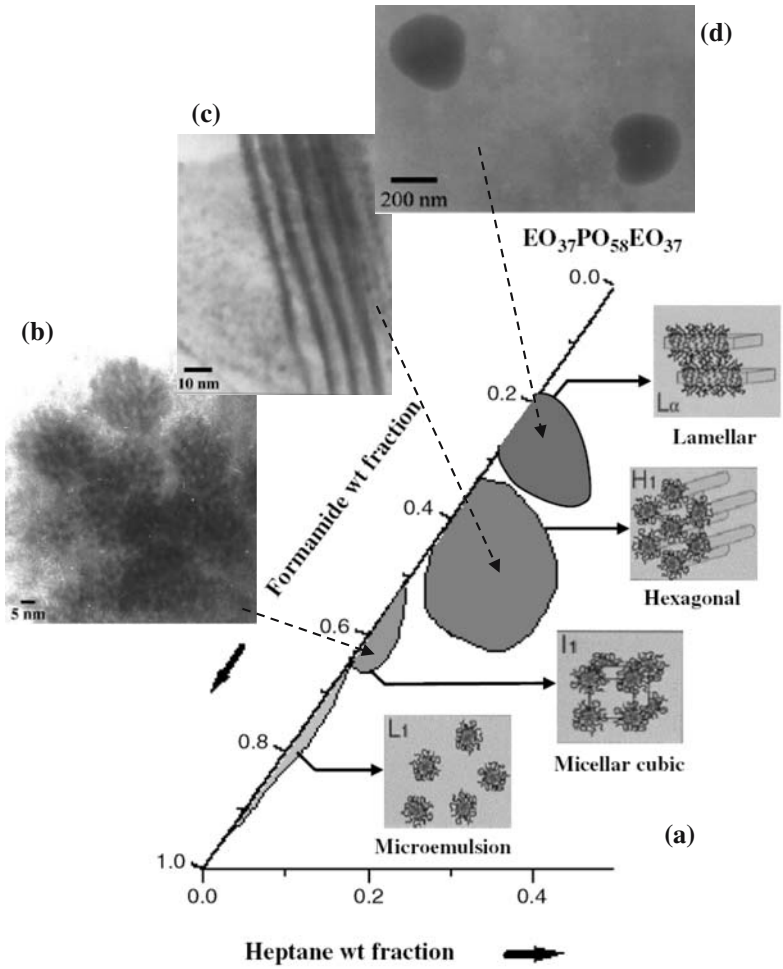

Fig. 10. Templated synthesis of ZnSe nanostructures using poly(ethylene oxide)-poly(propylene oxide)-poly(ethylene oxide) ($EO_{37}PO_{58}EO_{37}$) amphiphilic block copolymer as the surfactant: (a) Partial ternary isothermal phase diagram of the $EO_{37}PO_{58}EO_{37}$-heptane-formamide system at room temperature, (b) TEM images of 3 nm ZnSe quantum dots forming spherical domains consisting of a number of individual quantum dots synthesized inside the spherical nanodomains of the cubic micellar LC phase, (c) ZnSe nanowires with an average diameter of about 3 nm prepared in the hexagonal LC phase, and (d) ZnSe nanodiscs synthesized in lamellar phase. Reprinted from G. N. Karanikolos, P. Alexandridis, R. Mallory, A. Petrou, and T. J. Mountziaris, *Nanotechnology* **16**, 2372 (2005), [111] with permission from IOP Publishing Ltd.

demonstrated that the use of fluorinated monomers (such as heptadecafluorodecyl acrylate, HDFA) results in the formation of ordered polymeric structures not seen for their non-fluorinated counterparts (such as diacrylate, DA) [128]. The explanation for this phenomenon is that the fluorinated derivative has lower surface energies resulting in an enhanced segregation within the smectic layers [128]. Hence, the monomers remain trapped within the LC phase throughout the polymerization process, which results in the formation of ordered polymeric nanostructures (Fig. 11). Meanwhile, the non-fluorinated derivatives undergo phase separation from the LC phase after a period of time. The resultant random arrangement of the polymer in the phase-separated regions leads to the formation of polymeric nanostructures lacking order [128]. It was also noted that both fluorinated and aliphatic network structures phase-separate from the host LC while the linear fluorinated chain is retained.

As we will see later, thermotropic liquid crystalline phases provide significant utility for the organization of nanostructures through assisting with assembly processes. However, there are surprisingly few examples as of yet where the synthesis of metallic, semiconducting, or magnetic nanoparticles has been

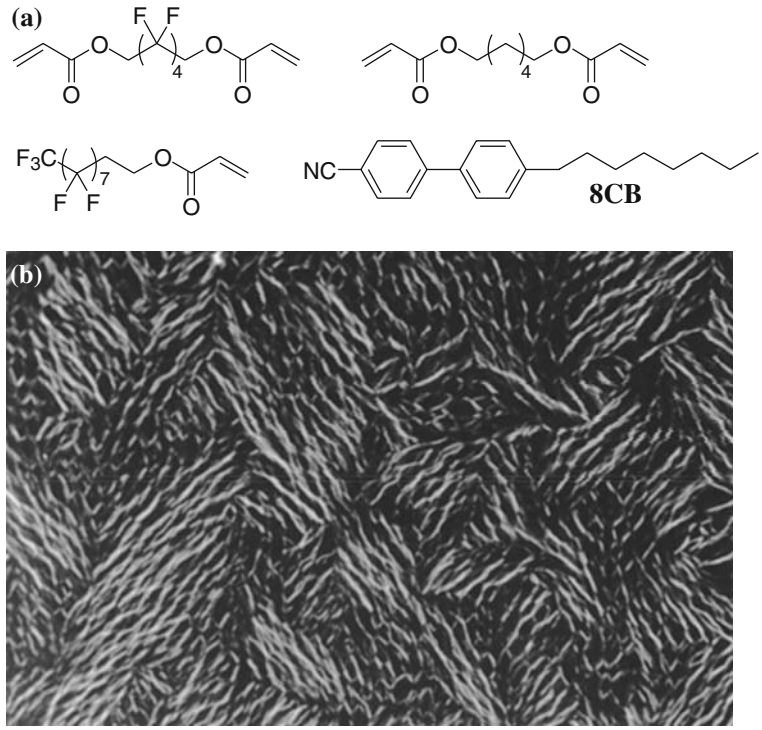

Fig. 11. (a) Monomer and LC structure of octafluorohexanediol diacrylate, hexanediol diacrylate, heptadecafluorodecyl acrylate, and the 4-cyano-4′-*n*-octyl-biphenyl (8CB) phase sequence on cooling (°C): Iso 40 N 32 SmA). (b) Optical texture (200×) of 4.9% poly-HDFA in 8CB obtained at 60 °C using a polarized microscope, demonstrating continued birefringence past the isotropic transition temperature (40 °C) of 8CB. Reprinted with permission from D. T. McCormick, R. Chavers, and C. A. Guymon, *Macromolecules* **34**, 6929 (2001), [129]. Copyright 2001 American Chemical Society.

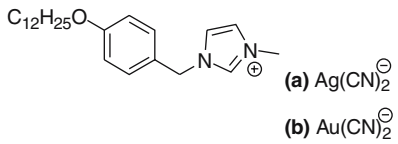

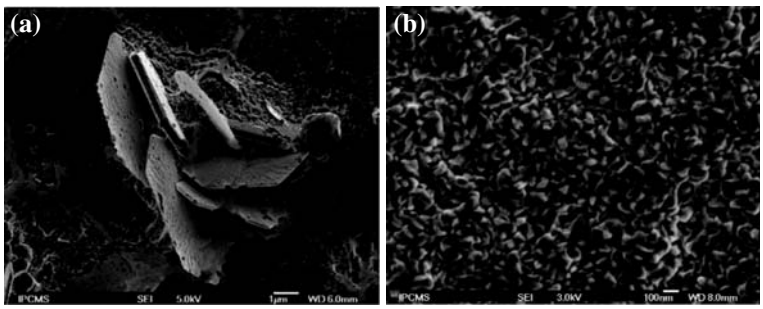

Fig. 12. Structure of imidazolium LC with dicyanoargentate(I) and dicyanoaurate(I) counter ion used as precursors for the fabrication of Au and Ag nanostructures by electrodeposition from the SmA phase: (a) hexagonal Ag platelets, and (b) leaflike Au forms. Reprinted with permission from W. Dobbs, J-M. Suisse, L. Douce, and R. Welter, *Angew. Chem., Int. Ed.* **45**, 4179 (2006), [132]. Copyright 2006 Wiley-VCH.

carried out in the condensed phase in a fashion analogous to that for lyotropic liquid crystals. Hence, further research in developing methods for the utilization of the condensed thermotropic LC phase for nanoparticle synthesis is likely to develop to a more intensively pursued research area in the near future, due to the potential of attaining shape and size-selective synthesis as well as self-assembly in one-pot.

One successful approach of making use of ionic liquid crystal precursors was recently presented by

Taubert for the synthesis of CuCl nanoplatelets using a lamellar ionic liquid crystal (however, in the isotropic liquid state) [131]. Shortly thereafter, this method was refined by Douce and co-workers to form leaf-like Au nanostructures as well as Ag nanoplatelets by electrodeposition from the lamellar LC phase of imidazolium LCs containing dicyanoargentate(I) or dicyanoaurate(I) counter ions (Fig. 12) [132]. Using another approach, Lattermann *et al*. succeeded in synthesising metallic Cu nanoparticles (3 nm in diameter) by reducing Cu(II) complexes of hexagonal columnar poly(propylene imine) (PPI) dendrimers, in addition to iron oxide nanoparticles (10--15 nm in diameter) [133] in analogy to reports using non-liquid crystalline dendrimers such as poly(amidoamine) (PAMAM) for the preparation of Au nanoclusters [134].

4. ASSEMBLY AND ORGANIZATION USING LCS

Self-assembly of metallic, magnetic, or semiconducting nanoparticles is a promising technique for preparing larger, organized structures because of its low cost, high yield, and ability to achieve extremely small features. Self-assembly of nanoparticles, a major goal for technological advances is essential for the integration and application of nanomaterials in high-tech devices. Most assembling methods lead to confined nanoparticle (NP) arrays, which do not allow for manipulation of the bulk organization. However, the specific properties and potentials of NPs will depend on whether they comprise periodic organized structures such as monolayer or multilayer films or are solutions of organized or randomly dispersed entities [135, 136], and whether they can rapidly respond to external stimuli or not. To produce periodic arrays of NPs, a variety of assembling strategies have been developed over the past years including immobilization on solid supports using molecular imprinting techniques [137], creation of films at air–water interfaces (Langmuir–Blodgett films) [138–143], or preparation of NP-filled polymer matrices [144]. Applying the concepts of supramolecular chemistry and molecular recognition of low molecular mass liquid crystals (LCs) to NP organization introduces means of control over the assembly of nanoscale systems into extended morphologies. In the past years, self-assembly of NPs into arrays has been successfully introduced through modification of nanoparticle systems with biomolecules (DNA, proteins) [145–151]. Other recognition elements include host-guest complexes, polymerizable functional groups, metal complex formation, H-bonding, and π–π stacking [152], with the latter two being as some of the main driving forces responsible for self-assembly in many lyotropic and thermotropic LC phases [11–13]. So far, the majority of studies involving LCs as templates or matrices for NP patterning, in particular for the synthesis of nanoscale materials, as discussed in the previous section employ lyotropic LC phases but rarely thermotropic phases.

Aside from the wealth of experimental and theoretical data on the formation of networks and chain-like particle aggregates in colloidal nematic dispersions based mainly on the formation of topological defects, this section will focus on anisometric nanomaterials forming LC phases, LC-coated nanoparticles, and 1-D nanostructures suspended in LC phases.

4.1. Nanomaterials forming LC phase morphologies

Anisotropic colloidal nanocrystals such as nanorods or nanodisks cannot only be synthesized using LC phases, but may also form the basis for a new class of mineral-based liquid crystal materials [153] which could have some unique and important properties such as high thermal stability, a well-defined rigid structure with weak interparticle attractions, and a very short range soft repulsion that might give rise to unique rheological properties [154].

Liquid crystalline ordering has been observed for a variety of rod-shaped nanoparticles in concentrated dispersions [155–157], at the air–water interface (Langmuir–Blodgett films) [158], and in evaporated films [159–165]. As an example, concentrated dispersions of CdSe nanorods have exhibited both nematic (Fig. 13) [155] and smectic-like ordering [157]. In analogy to the classical molecular shapes of organic LCs, disk-shaped nanoparticles (nanodisks or nanoplatelets) should also exhibit orientational ordering at sufficient concentrations, as well as sufficiently narrow size and shape distributions [166, 167]. Recent examples include dispersions and films of submicrometer-size colloidal disks of $Al(OH)_3$, $Ni(OH)_2$, and phosphatoantimonate ($H_3Sb_3P_2O_{14}$) sheets forming in part nematic, smectic, and columnar type mesophases [168–172]. For instance, sterically stabilized colloidal CuS nanodisks (14–20 nm in diameter, thickness of about 5 nm) have recently been shown to form self-assembled columnar structures with exten-

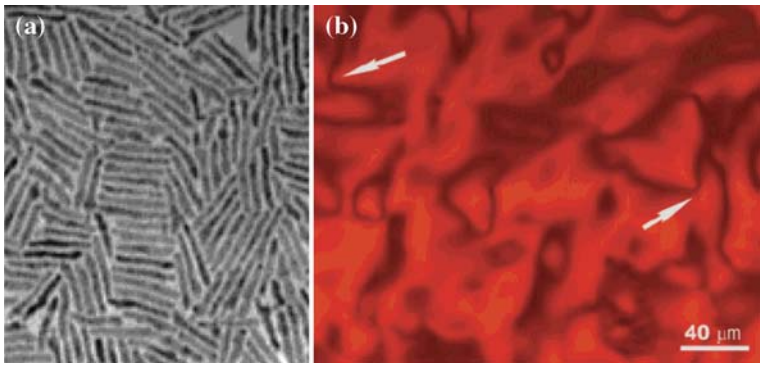

Fig. 13. (a) Transmission electron micrograph of CdSe nanorods with width of ca. 4.2 nm and length of 40 nm. (b) Images of liquid crystalline phase in concentrated solution of CdSe nanocrystals under a polarized light optical microscope. Disclinations of strength of ½ are clearly visible (the arrows point to the disclinations). Reprinted with permission from L. Li, J. Walda, L. Manna, and A. P. Alivisatos, *Nano Lett*. **2**, 557 (2002), [155]. Copyright 2002 American Chemical Society.

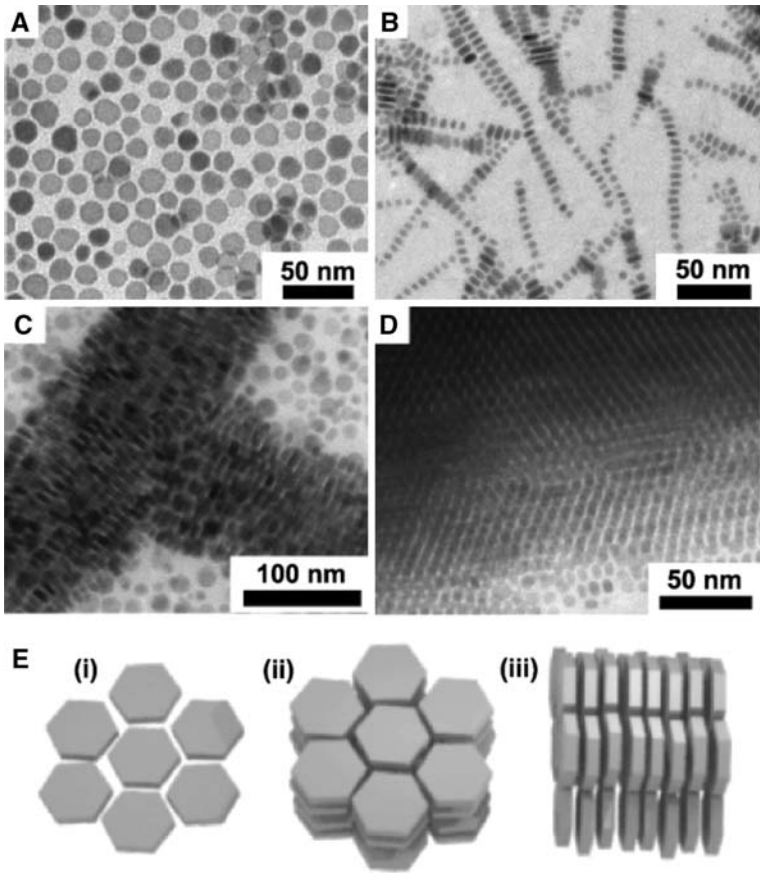

Fig. 14. TEM images of CuS and Cu_2S nanodisks. (A) CuS nanodisks in a monolayer on their faces. (B) Linear chains of stacked Cu_2S nanodisks. (C) CuS nanodisks crystallized into a "T"-shaped structure. (D) Ordered Cu_2S nanodisk assembly oriented parallel to the substrate. (E) Illustrations of different nanodisk assemblies and orientations on the substrate: (i) a monolayer; (ii) hexagonal columnar assembly with columns oriented perpendicular to the substrate; (iii) columnar assembly with columns oriented parallel to the substrate. Reprinted with permission from A. E. Saunders, A. Ghezelbash, D.-M. Smilgies, M. B. Sigman Jr., and B. A. Korgel, *Nano Lett*. **6**, 2959 (2006), [154]. Copyright 2006 American Chemical Society.

sive hexagonal closed packing (Fig. 14) [154]. Additionally, several examples have appeared in the literature where electron microscopy images of evaporated films of nanodisks have hinted at long-range orientational ordering, i.e. LC-like organization of nanodisks [173–177].

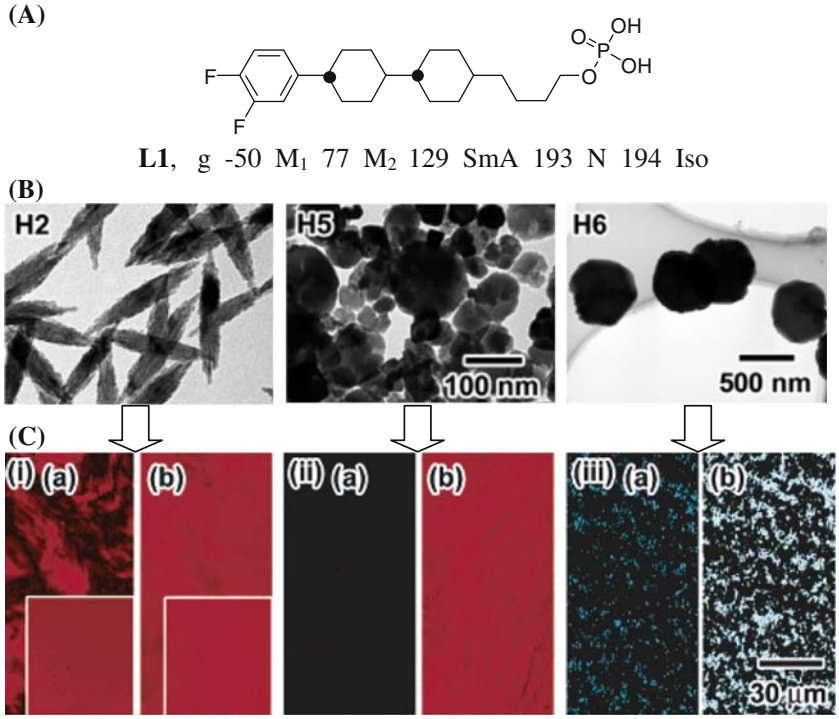

Fig. 15. (A) Structure of the LC phosphate (**L1**) used to prepare α-Fe_2O_3/LC hybrids, (B) TEM images of the α-Fe_2O_3 particles **H2**, **H5**, and **H6** with rod-like, polydisperse, and hexagonal platelet shape, respectively. (C) Optical photomicrographs of thermotropic hybrid LC phases of 1/2 hybrids (i.e. ratio L/H = 1/2, w/w) of (i) nematic-like **L1**/**H2**, (ii) non-LC **L1**/**H5**, and (iii) non-LC **L1**/**H6** at 90 °C (a) with a polarizer, (b) without polarizer; insets in (i) are sheared monodomains. Another hybrid with cuboidal α-Fe_2O_3 particles (not shown) was reported to show a cubic-like LC phase as indicated by small angle x-ray scattering. Reprinted with permission from K. Kanie, and M. Muramatsu, *J. Am. Chem. Soc.* **127**, 11578 (2005), [187]. Copyright 2005 American Chemical Society.

4.2. LC-decorated nanoparticles

We have just seen that metallic, semiconductor and mineral-based nanomaterials are capable of forming LC phases (or at the very least long-range orientational ordering) without the aid of organic mesogens. Clearly, this phenomenon is limited to nanomaterials with a pronounced anisometric shape (high aspect ratio), but what about spherical nanoparticles? One methodology that has proven to be successful in achieving liquid crystallinity for mineral- or metal-based nanomaterials is based on decorating small, spherical nanoclusters with thermotropic mesogenic or pro-mesogenic molecules (formation of a monolayer). There are several recent examples, where self-assembly of quasi-spherical gold nanoparticles into LC phase morphologies has been successful using thermotropic LC capping agents, giving rise to nematic or smectic phase morphologies [178–182]. A typical procedure using gold nanoparticles as an example involves utilization of the Brust–Schiffrin method in the presence of thiolated thermotropic LCs to functionalize the gold nanocluster surface. However, caution is warranted when designing liquid crystalline gold nanoclusters. While gold nanoclusters are generally considered to be stable to air and moisture, as well as to temperatures up to ca. 120 °C if the hydrocarbon chain of the thiol ($C_nH_{2n+1}SH$) is equal or longer than 12 carbon atoms ($n \geq 12$) [183], gold nanoclusters in the size regime of conventional LC molecules (around 2 nm) are known to undergo size changes with increasing temperature. The reason for this size-effect was explained by the fact that smaller nanoclusters have larger chemical potentials and, as a result thereof, have a greater tendency to sinter and increase in size (Ostwald ripening) releasing thiols from the surface [184, 185].

Apart from spherical metal nanoclusters, Kanie *et al.* also reported on the formation of thermotropic nematic and cubic phases by coating needle-shaped TiO_2 particles, as well as α-Fe_2O_3 and SiO_2-coated Fe_3O_4 nanorods or -platelets (Fig. 15) [186–188].

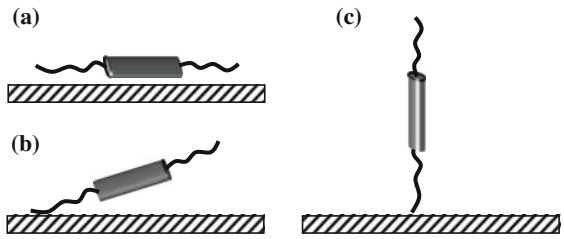

Fig. 16. Specific interactions (or coupling) of LC molecules with different or modified surfaces can result in (a) planar (enforced, for example by polyimide alignment layers), (b) tilted (found for certain glass surfaces) or (c) homeotropic anchoring (enforced by treatment of glass surfaces with surfactants).

4.3. 1-D nanomaterials suspended in thermotropic LCs

The organization, orientation, and re-orientation, of anisometric 1-D nanostructures using thermotropic LCs has been the focus of much current research, particularly due to the prospect of controlling the order in such systems leading to new optical as well as electro-optical applications. Thermotropic LCs, especially low-molecular mass thermotropic LCs, offer tremendous advantages over conventional liquid media for the organization and switching (re-orientation) of 1-D nanomaterials. In addition to intrinsic anisotropic properties (e.g., dielectric anisotropy, $\Delta\varepsilon$), specific interactions or coupling with surfaces such as planar, tilted, or homeotropic anchoring (see Fig. 16), thermotropic LCs are characterized by orientational ordering that can be manipulated by external electric or magnetic fields commonly with relatively short response times (high switching speed).

The first successful attempt of using thermotropic LCs for producing organized nanomaterial arrays on surfaces was demonstrated by Patrick and co-workers (Fig. 17) [189]. In the method, termed liquid crystal imprinting (LCI), nanometre-sized building blocks are dissolved in a non-chiral nematic LC under an applied magnetic field or alternatively using rubbed polymer alignment layers (commonly used in LC device technologies). In this way, the aligned nematic LC phase imposes (imprints) its uniform orientation onto the 1-D nano-building blocks (up to macroscopic length scales), resulting in organized thin films deposited onto the supporting substrate. The usefulness of this method to other more diverse systems and its limitations has recently been reviewed by Patrick *et al.* [190].

Other examples of controlling the orientation of anisotropic nanomaterials using thermotropic nematic LCs include the levitation of nickel nanowires in a twisted nematic cell [191, 192] and parallel alignment

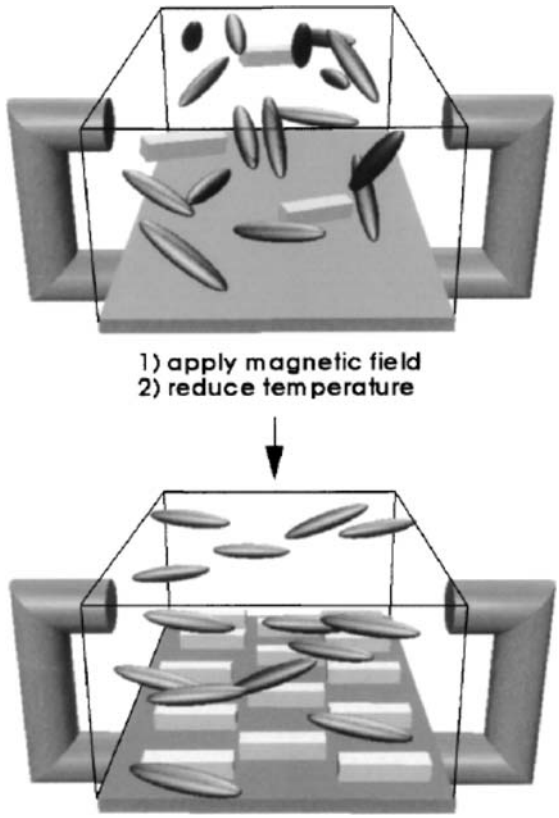

Fig. 17. Demonstration of the principle of the formation of uniaxial molecular films by liquid crystal imprinting (LCI) in a magnetic field. Reprinted with permission from J. Mougous, R. Baker, and D. L. Patrick, *Phys. Rev. Lett.* **84**, 2742 (2000), [189]. Copyright 2000 by the American Physical Society.

of single-wall as well as multi-wall carbon nanotubes (CNT) in low-molecular mass nematic LCs [193–195] (Fig. 18) and nematic elastomers [196]. These examples clearly demonstrate the high potential for the use of such composites as electromechanical actuators [196]. Patrick and co-workers also demonstrated that control over the alignment of elongated nanoparticles in nematic LCs could be extended to needle-shaped, micron-sized semiconducting SiC particles (10–100 μm in length), and showed that the equilibrium orientation largely depends on the particle's surface chemistry (e.g. modification of anchoring conditions from parallel to homeotropic *via* particle surface modification with octadecyltrichlorosilane, OTS) as well as the choice of LC [197]. Another approach presented by the same group produces highly oriented films of single- and multi-wall CNTs by casting a suspension of these particles through a porous membrane using LCs as a solvent [198]. Organized arrays of high aspect ratio carbon nanostructures such as nanotubes (CNTs) and nanofibers have also

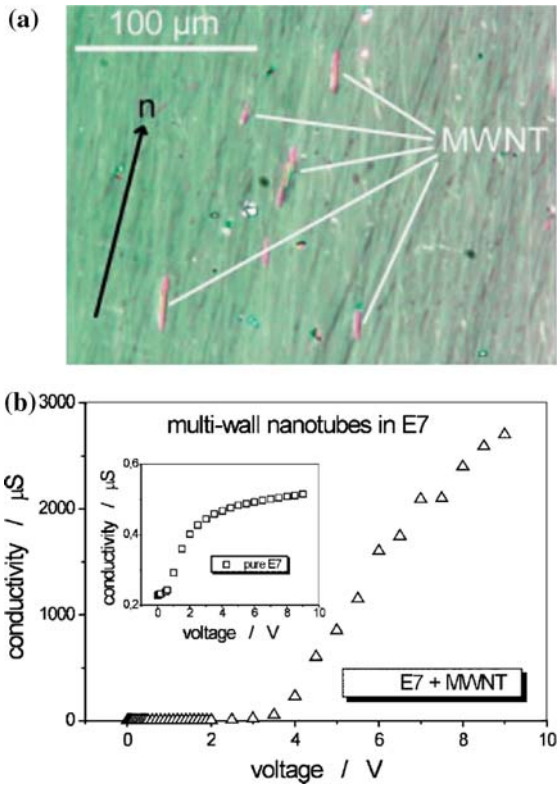

Fig. 18. (a) Polarized optical photo micrograph of multi-wall carbon nanotubes (MWNT) in a room-temperature N mixture (E7, Merck) confined in a 6 micron sandwich cell (large magnification). (b) Increased conductivity of the E7/WWNT mixtures in comparison to pure E7. Reprinted with permission from I. Dierking, G. Scalia, P. Morales, and D. LeClere, *Adv. Mater.* **16**, 865 (2004), [193]. Copyright 2004 Wiley-VCH.

been fabricated by Crawford *et al.* using lyotropic [199] as well as high molecular mass thermotropic LCs [200, 201].

Recent numerical calculations (potential of mean force, PMF) for defect structures that arise when spherocylindrical (anisotropic rod-like) nanoparticles are immersed in a bulk nematic LC were used to analyze different configurations (including triangular, linear, and parallel with respect to their long axis) of the anisometric particles with strong homeotropic anchoring at their surfaces. Comparing the attractive interactions between elongated and spherical nanoparticles, de Pablo *et al.* showed that similar interparticle energies result for linear arrays, in contrast to 3.4 times stronger interactions for the spherocylinders in a triangular as well as parallel array [202]. These numerical results indicate that under equal anchoring conditions, elongated rod-like nanoparticles (CNTs, nanowires, or nanorods) in a nematic phase interact with one another preferentially forming parallel arrays, in comparison to chain-like (linear) arrays formed by spherical particles, as discussed in more detail in the next section.

5. DEFECT FORMATION IN LC SUSPENSIONS

The capability of orienting small particles using thermotropic liquid crystals has been known for more than 35 years [203]. So far, topological defects (and the formation of particle aggregates as a result thereof) have been most intensively studied for nematic and chiral nematic LCs [204], and much of the underlying physics has recently been reviewed by Stark [205]. An interesting example of nanoparticles in cholesteric LCs has recently been presented by Mitov *et al.* [206, 207]. The authors showed that Pt nanoclusters are capable of mimicking the typical fingerprint textures of chiral siloxane LC oligomers (Fig. 19).

Dispersed colloidal particles disrupt the nematic order, and minimization of the elastic energy leads to the formation of anisotropic colloidal structures [208]. Depending on the strength and direction of the nematic anchoring on the particle surface, sufficiently large particles can form various types of topological defects such as Saturn rings, hyperbolic hedgehogs, and boojums (Fig. 20) in agreement with theoretical considerations [209–215]. Experimental studies focused on dispersions of water microdroplets [208, 216, 217], ferrofluid [218], gold coated glass spheres [219], or silicon oil [220–223] in nematic LCs as well as latex particles in lyotropic LCs [217, 224].

For most particles, if the nematic LC molecules are strongly and perpendicularly anchored at the surface of a spherical particle, the particles act like a radial hedgehog carrying a topological charge. Placed in a uniformly aligned nematic solvent to satisfy the boundary conditions at infinity, the particle should nucleate a further defect in its nematic environment. As theoretically predicted [225–227], the dipole is the preferred configuration for large particles and sufficiently strong anchoring, although quadrupoles are also observed [219]. The topological dipole formed by one quasi-spherical particle and an accompanying topological defect, known as a hyperbolic hedgehog, generate elastic forces that lead to the formation of chain-like particle aggregates [228], even when confined in microcapillaries (Fig. 21) [229]. However, the interactions between colloidal particles and the nematic LC molecules strongly depend on the particular combination of the two materials, the molecular structure and elastic properties of the LC, as well as

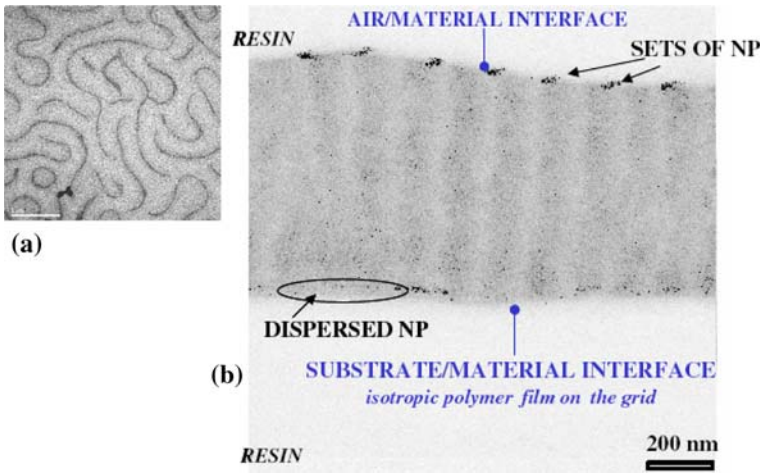

Fig. 19. (a) TEM micrograph of cholesteric siloxane LC oligomer doped with Pt nanoparticles (1.5 wt%); scale bar: 1 μm. Particle assemblies are structured into ribbons mimicking the fingerprint texture. (b) TEM micrograph of a cross-section. Reprinted from M. Mitov, C. Bourgerette, and F. de Guerville, *J. Phys. Condens. Matter* **16**, 1981 (2004), [207] with permission from IOP Publishing Ltd.

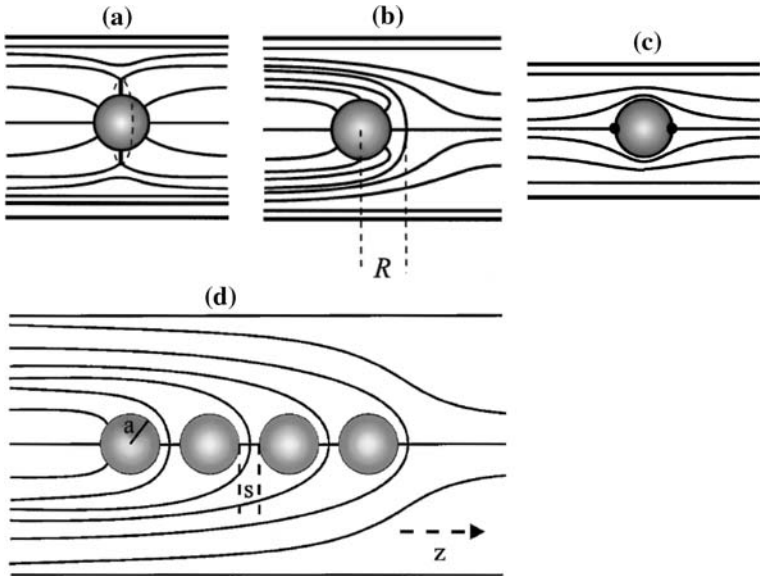

Fig. 20. Typical defects created by spherical particles in nematic LCs: (a) hyperbolic hedgehog as a particle with normal boundary conditions is introduced in a homogeneously aligned LC. The droplet defect pair has a total topological charge of zero, and dipolar symmetry. (b) The director field of a Saturn ring, a disclination loop of strength -½. The total topological charge is zero. (c) A particle with planar boundary conditions in an aligned LC. Two surface defects known as boojums are induced on the surface of the particle. (d) Schematic representation of the director field for a chain of droplets formed by interaction between the topological dipoles [shown in (b)]. There are exactly as many defects as particles. Reprinted with permission from P. Poulin and D. A. Weitz, *Phys. Rev. E***57**, 626 (1998), [216]. Copyright 1998 by the American Physical Society.

on the type, size [230], and shape of the colloidal particle used. For example, gold nanoclusters in the size regime between 1 and 5 nm coated with either aliphatic and/or chiral aromatic thiolates promote homeotropic anchoring of nematic LC molecules to the particle surface, and are capable of forming topological defects (i.e. dipoles and hyperbolic hedgehogs) generating elastic forces in the N-LC that lead to the formation chain-like particle aggregates. These aggregates are responsible for birefringent stripe domains visible in thin-film textures by polarized optical micrsocopy (POM, see Fig. 22), which are separated by homeotropic domains produced by randomly distributed particles residing at the glass/

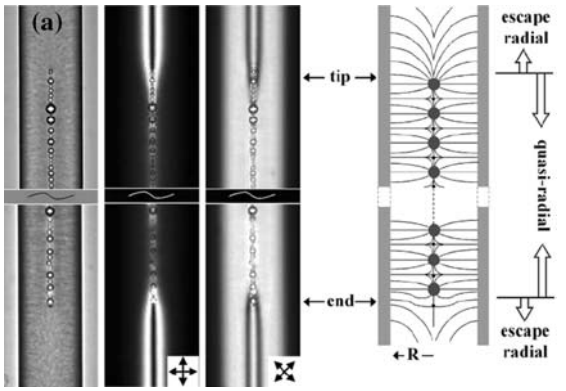

Fig. 21. Polymer droplets forming chains in a nematic phase confined in a microcapillary. The escape-radial configuration inside the capillary (schematically shown on the right) was stabilized by treating the inner surfaces of the capillary with a lecithin surfactant to enforce homeotropic anchoring. Microscope images of the structure in white light and between cross polarizers. The directions of polarizers are indicated. Reprinted with permission from P. Kossyrev, M. Ravnik and S. Žumer, *Phys. Rev. Lett.* **96**, 048301 (2006), [229]. Copyright 2006 by the American Physical Society.

N-LC interfaces [231]. In principle, such a device could serve as excellent model systems for LC-based sensors with improved sensitivity as those described by Guzmán and co-workers [232]. In additon to the formation of birefringent stripe domains, similar to cholesteric finger textures (or because of the chiral thiolate capping the nanocluster), the chiral modifield nanoparticles induce a chiral nematic phase (N*) in the non-chiral N-LC host [231]. A related separation effect into particle-poor and particle-rich domains was also found for functionalized gold nanoclusters in bolaamphiphilic LCs. In this case, polar, hydrophilic gold nanoclusters in the particle-rich domains stabilized the columnar phase of one of the LCs used [233].

Strongly related, although not for nanoscale particles, Lev and Lavrentovich *et al.* have reported on the formation of dense hexagonal structures in addition to chain-like aggregates as a result of both repulsive and attractive interactions between glycerol droplets at the nematic/air interface (Fig. 23) [234, 235]. Finally, the formation of cellular networks in suspensions of colliodal polymethylmethacrylate (PMMA) particles in N-LCs was described by by a number of groups [236–240] as a result of spatial separation into particle-rich and particle-poor domains during slow cooling past the isotropic/nematic phase transition temperature. It was also pointed out that slow liberation of alkane remnants from the PMMA particles is critical for this network formation process [240].

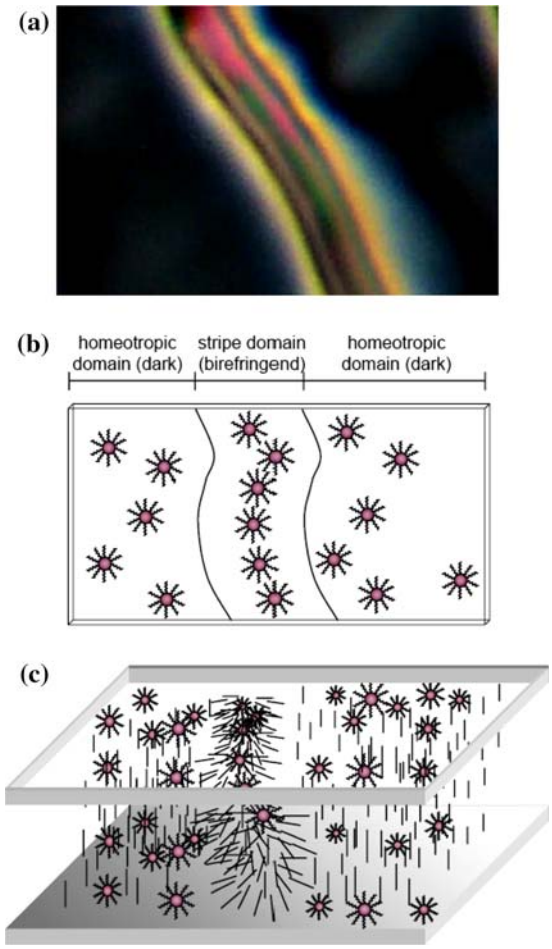

Fig. 22. Model for the organization of the gold nanoparticles in the N-LCs. (a) Isolated stripe domain (centre) between two homeotropically aligned domains (left and right); (b) top view indicating particle-rich (stripe domain) and particle-poor areas (homeotropic domains) – LC molecules are omitted for clarity; and (c) 3D model with gold nanoclusters residing at both glass/N-LC interfaces in the homeotropic domains. From H. Qi, and T. Hegmann, *J. Mater. Chem.* **16**, 4197 (2006), [231]. Reproduced with permission from The Royal Society of Chemistry.

6. APPLICATIONS

Drawing from the wealth of theoretical and experimental work, and further stimulated by an ever increasing variety of new nanomaterials differing in size, shape, and properties, there has been a surge to develop and improve upon existing or open up avenues for new technological applications of colloidal LC suspensions, for example for light scattering devices and flat panel display applications.

Likely one of the most intensively pursued materials combinations falls in the group of so-called filled nematics, which started out with suspensions of

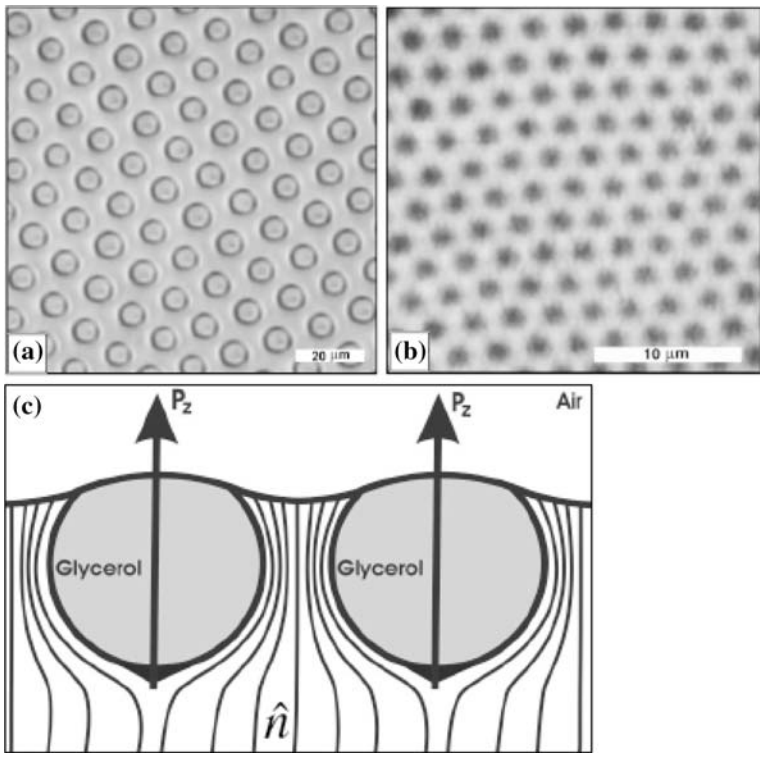

Fig. 23. Optical microscopy pictures of hexagonal structures at the free surface of the thick nematic layer, formed by droplets of different average diameter: (a) $D = 7$ μm; (b) $D = 1$ μm. (c) Schematic drawing of the director field in the top part of the LC layer. Reprinted with permission from I. I. Smalyukh, S. Chernyshuk, B. I. Lev, A. B. Nych, U. Ognysta, V. G. Nazarenko, and O. D. Lavrentovich, *Phys. Rev. Lett.* **93**, 117801 (2004), [235]. Copyright 2004 by the American Physical Society.

fine particles (not necessarily at the nanoscale), such as aerosils [241–243] or titanium dioxide particles [244] in a nematic LC matrix. Along with the 'nano-revolution', the past few years have seen a steady increase in the use of nanoscale colloidal particles [245, 246]. The intensive light scattering of such filled nematics in the field-Off state is mainly caused by a large number of orientational defects generated by the dispersed particles, as discussed in the previous section. In the field-On state, the sandwiched film of the filled nematic becomes transparent due to the orientation of the nematic LC molecules with the external electric field (Freedericksz transition [247]). A specific property of filled nematics is the residual transmittance after the field is switched off (memory effect) [248]. The same switching process between opaque and transparent has recently been described for nanoparticle networks embedded in nematic LCs as an all-mechanical process using low frequency shearing micro-vibrations [249]. However, it is often found that the electro-optical performance of such filled nematics strongly depends on the physical and chemical properties of both the LC and the filler particles, the concentration, as well as on the parameters of the applied electric field [250].

Müller *et al*. demonstrated electrically controlled light scattering by embedding quasi-spherical gold nanoparticles (80 nm in diameter) in a nematic LC mixture [251]. Their experiments showed that spherical gold nanoclusters behave optically like spheroidal particles when suspended in anisotropic materials (near-field spectral tuning) such as nematic LCs. Park and Stroud confirmed these experimental findings and calculated that gold nanoclusters embedded within a thin film of a nematic liquid crystal could indeed enhance the surface plasmon splitting through deformations of the director orientation by the nanoparticle surface [252]. Since the transmission and absorption of such systems could be tuned by applying an electric field, or by controlling the surface interactions between the metal nanocluster and the N-LC, such N-LC embedded metal nanoclusters could form the basis for new electro-optical materials. Kossyrev and co-workers later extended this approach to gold nanodot arrays formed on one glass substrate of a sandwiched nematic LC cell with far-

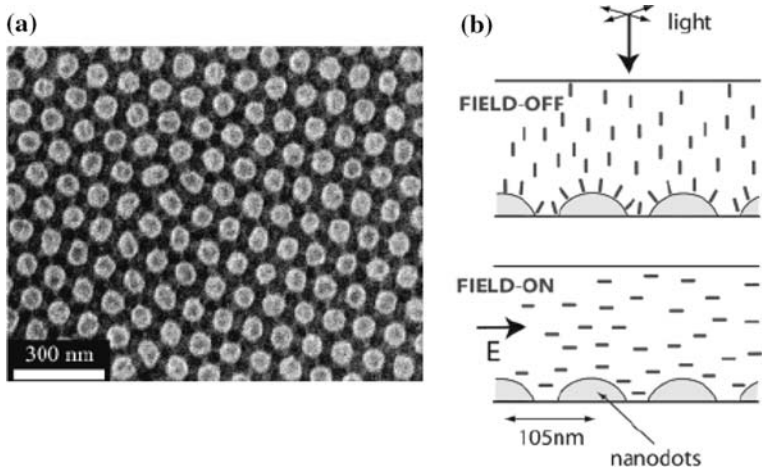

Fig. 24. (a) SEM image of nanostructured array of gold nanodots. (b) Geometry of gold nanodot arrays in a LC cell with a metallic Bragg grating as a top interdigitated electrode (not shown). The idealized direction of electric field between interdigitated electrodes, *E*, is indicated. The molecular orientation of liquid crystal is schematically depicted. Reprinted with permission from P. A. Kossyrev, A. Yin, S. G. Cloutier, D. A. Cardimona, H. Danhong, P. M. Alsing, and J. M. Xu, *Nano Lett*. **5**, 1978 (2005), [253]. Copyright 2005 American Chemical Society.

field spectral tuning, resulting in a proof-of-concept device capable of voltage dependent colour tuning (Fig. 24) [253].

Further electro-optical effects were also reported for other LC nanocomposites, such as small memory effects in clay mineral/nematic mixtures [254], an optically ''hidden'' electrophoretic effect, polarity-controlled bistable and multistable switching [255], lower Freedericksz transition voltages in nematic LCs doped with either CdSe nanorods [256] or ferroelectric nanoparticles [257], and lower operating voltages as well as shorter response times in different LCD switching modes using nanoscale MgO particles [258].

In this sense, LCs, which by themselves are among the most interesting electro-optical materials, are also explored as a filler material for two- and three-dimensional photonic band gap structures such as synthetic porous opals [259, 260].

Surprisingly, examples dealing with nanoparticle-filled smectic phases are rather rare considering the large number of examples exploring the electro-optical properties of filled nematics. This likely arises from the fact that comparatively little is known about nanoparticle interactions in smectic [261] and higher ordered LC phases, apart from so-called ferrosmectics [262–265] (smectic phases filled with magnetic nanoparticles) dating back to the early work of de Gennes [203]. Matsui and Yasuda reported on using amorphous TiO_2 nanoparticles (17 nm in diameter) randomly dispersed in a ferroelectric LC mixture (based on the SmC*), and demonstrated the usefulness of such mixtures for video-rate grey-scale FLC devices [266].

Another rare use of nanostructured LC-based materials, not focusing on device or display applications, was recently published by Gin *et al*., demonstrating the use of nanostructured, enantioselective Diels-Alder catalysts *via* acid-induced LLC assembly followed by in situ photopolymerization [267].

7. CONCLUSIONS

The reproducible synthesis of nanoscale devices is becoming increasingly important due to their critical role in the creation of a vast array of technological devices. The creation of nanostructured mesoporous materials has been an important issue for quite some time due to their implications for fuel cells, automotive emission controls, and various catalytic applications such as hydrogenation reactions. Lyotropic liquid crystals have been successfully used as templates for the synthesis of mesoporous nanostructures with a uniform pore size and shape composed of many different metals.

LLCs have also been used for the synthesis of spherical nanoparticles and high aspect ratio nanorods. The LLC phase itself is seeing an increasing use as a 'nanoreactor' for the synthesis of nanomaterials of uniform size and shape.

Although thermotropic liquid crystals have not yet been used to a great extent for the synthesis of metallic, magnetic, or semi-conducting nanoparticles,

the condensed phase provides an excellent medium for attaining ordered polymeric nanostructures. In addition, there are numerous recent examples where the self-assembly of spherical nanoparticles has been successfully achieved utilizing condensed thermotropic phases. Thus, future work involving thermotropic liquid crystalline phases will provide many exciting challenges for achieving synthesis and self-assembly of nanoparticles with a uniform size and shape distribution, all in one-pot. Research in this area will likely expand employing many different molecular LC shapes and phase morphologies including disk-like, bent-core and multi-block LCs, since most reports so far dealt with thermotropic nematic and smectic modifications.

To conclude, the design of functional liquid crystal nanocomposites has and will further contribute to the nanotechnology revolution, and likely to the discovery or improvement of many high-tech applications in areas such as nanoscale electronics, electro-optics, sensors, optical memories, and display devices. Particularly in the field of LC displays—an industry worth more than $60 billion/year—one could expect tendencies towards new switching modes, lower operating voltages, faster switching speeds, and higher contrast ratios—enormous advantages in a world with more LCDs than people [268].

ACKNOWLEDGMENTS

The authors thank the Natural Sciences and Engineering Research Council (NSERC) of Canada and the University of Manitoba for financial support.

REFERENCES

1. B. Bhushan, ed. *Handbook of Nanotechnology* (Springer 2004).
2. G. Ozin and A. Arsenault*Nanochemistry—A Chemical Approach to Nanomaterials* (Cambridge, RSC, 2005).
3. G. Cao*Nanostructures & Nanomaterials: Synthesis, Properties & Applications* (Imperial College Press, London, 2004).
4. C. N. R. Rao, G. U. Kulkarni, P. J. Thomas, and P. P. Edwards, *Chem. Soc. Rev.* **29**, 27 (2000).
5. M. Sarikaya, C. Tamerler, A. K.-Y. Jen, K. Schulten, and F. Baneyx, *Nat. Mater.* **2**, 577 (2003).
6. G. Cao and C. J. Brinker, eds. *Annual Report of Nano Research*, Vol. 1 (World Scientific Publishing, 2006).
7. G. W. Gray, in *Handbook of Liquid Crystals*, Vol. 1, D. Demus, J. Goodby, G. W. Gray, H. W. Spiess, and V. Vill, eds., (Wiley-VCH, Weinheim, 1998), pp. 1–16.
8. B. Bahadur eds., *Liquid Crystals-Application and Uses* (1–3World Scientific, Singapore, 1990).
9. D. Demus, and J. Goodby, and G. W. Gray, and H.W. Spiess, and V. Vill eds., *Handbook of Liquid Crystals* (1Wiley-VCH, Weinheim, 1998) 731–896.
10. P. Collings and M. Hird, Introduction to Liquid Crystals (Taylor & Francis, 1997).
11. C. Tschierske, *Prog. Polym. Sci.* **21**, 775 (1996).
12. C. Tschierske, *J. Mater. Chem.* **8**, 1485 (1998).
13. C. Tschierske, *Annu. Rep. Prog. Chem., Sect. C* **97**, 191 (2001).
14. J. M. Seddon and R. H. Templer, In: Handbook of Biological Physics, Vol 1, R. Lipowsky and E. Sackmann, eds. (Elsevier, 1995), pp. 97.
15. D. Demus, and J. Goodby, and G. W. Gray, and H. W. Spiess, and V. Vill eds., *Handbook of Liquid Crystals* (3Wiley-VCH, Weinheim, 1998) 1–302.
16. M. Warner and E. M. Terentjev, *Liquid Crystal Elastomers* (Oxford University Press, 2003).
17. P. Xie and R. Zhang, *J. Mater. Chem.* **15**, 2529 (2005).
18. J. Barberá, B. Donnio, L. Gehringer, D. Guillon, M. Marcos, A. Omenat, and J. L. Serrano, *J. Mater. Chem.* **15**, 4093 (2005).
19. I.M. Saez and J.W. Goodby, *J. Mater. Chem.* **15**, 26 (2005).
20. T. Kato, *Science* **295**, 2414 (2002).
21. Mesophases that are characterized by long range positional and no orientational ordering are referred to as disordered crystals or plastic crystals. See P. A. Winsor, *Liquid Crystals & Plastic Crystals*, G. W. Gray and P.A. Winsor, eds., Vol. 1, (Horwood, Chichester, 1974),pp. 48.
22. D. Demus, J. Goodby, G. W. Gray, H. W. Spiess and V. Vill, eds., *Handbook of Liquid Crystals*, Vol. 2a, chpt. III,(Wiley-VCH, Weinheim, 1998), pp. 47–302 and S. Chandrasekhar, Vol. 2b, pp. 749–780.
23. H. Coles, in *Handbook of Liquid Crystals*, D. Demus, J. Goodby, G. W. Gray, H. W. Spiess, and V. Vill, eds., Vol. 2a (Wiley-VCH, Weinheim, 1998), pp. 335–410.
24. There exist several tilted and non-tilted smectic modifications, some of which are designated crystal phases, with a varying degree of in-plane ordering. For more details see ref [25].
25. G. W. Gray and J. W. Goodby, *Smectic Liquid Crystals: Textures and Structures* (Thompson Sci., 1984).
26. Higher ordered (tilted and non-tilted) smectic phases (and chiral versions thereof) have no equivalent in lyotropic LC phase morphologies.
27. S. Garoff and R. B. Meyer, *Phys. Rev. Lett.* **38**, 848 (1977).
28. S. Garoff and R. B. Meyer, *Phys. Rev. A* **19**, 338 (1979).
29. For an example of atropisomeric chiral dopants see: T. Hegmann, M. R. Meadows, M. D. Wand and R. P. Lemieux, *J. Mater. Chem.* **14**, 185 (2004).
30. C. S. Hartley, N. Kapernaum, J. C. Roberts, F. Giesselmann and R. P. Lemieux, *J. Mater. Chem.* 16, 2329 (2006), and references therein.
31. W. Hall, J. Hollingshurst and J. W. Goodby, in *Handbook of Liquid Crystal Research*, P. J. Collings and J. S. Patel, eds. (Oxford University Press, New York, 1997).
32. N. A. Clark and S. T. Lagerwall, *Appl. Phys. Lett.* **36**, 899 (1980).
33. D. M. Walba, in *Advances in the Synthesis and Reactivity of Solids*, T.E. Mallouck, ed. (JAI Press Ltd, Greenwich CT, 1991).
34. R. P. Lemieux, *Acc. Chem. Res.* **34**, 845 (2001).
35. J. W. Goodby, *Curr. Opin. Coll. Interf. Sci.* **7**, 326 (2002).
36. S. Chandrasekhar and G. S. Ranganath, *Rep. Prog. Phys.* **53**, 57 (1990).
37. S. Kumar, *Chem. Soc. Rev.* **35**, 83 (2006).
38. For an example see: T. Hegmann, B. Neumann, R. Wolf and C. Tschierske, *J. Mater. Chem.* **15**, 1025 (2005), and references therein.
39. J. L. Serrano*Metallomesogens* (Weinheim, VCH, 1996).

40. B. Donnio and D. W. Bruce, in *Structure and Bonding 95: Liquid Crystals II*, D. M. P. Mingos, ed. (Springer, Berlin, 1999) pp. 193.
41. For an example of macrocyclic LCs see: T. Hegmann, J. Kain, S. Diele, B. Schubert, H. Bögel and C. Tschierske, *J. Mater. Chem.* 13:991 (2003).
42. A. Pegenau, T. Hegmann, C. Tschierske, and S. Diele, *Chem Eur. J.* **5**, 1643 (1999).
43. H. Zheng and T. M. Swager, *J. Am. Chem. Soc.* **116**, 761 (1994).
44. X. Zeng, G. Ungar, Y. Liu, V. Percec, A. E. Dulcey and J. K. Hobbs, *Nature* 428, 157 (2004) and references therein.
45. B. Chen, X. Zeng, U. Baumeister, G. Ungar and C. Tschierske, *Science* 307, 96 (2005) and references therein.
46. For a recent example see: B. Bilgin-Eran, C. Tschierske, S. Diele and U. Baumeister, *J. Mater. Chem.* **16**, 1136 (2006).
47. For extensive work on fluorinated multi-block LCs and an extensive list of references describing the use of semi-fluorinated alkyl chains in LC design see: X. Cheng, M. Prehm, M. K. Das, J. Kain, U. Baumeister, S. Diele, D. Leine, A. Blume and C. Tschierske, *J. Am. Chem. Soc.* **125**, 10977 (2003).
48. T. Niori, T. Sekine, J. Watanabe, T. Furukawa, and H. Takezoe, *J. Mater. Chem.* **6**, 1231 (1996).
49. M. B. Ros, J. L. Serrano, M. R. Fuente, and C. L. Folcia, *J. Mater. Chem.* **15**, 5093 (2005).
50. R. A. Reddy and C. Tschierske, *J. Mater. Chem.* **16**, 907 (2006).
51. D. A. Coleman, J. Fernsler, N. Chattham, M. Nakata, Y. Takanishi, E. Korblova, D. R. Link, R.-F. Shao, W. G. Jang, J. E. Maclennan, O. Mondainn-Monval, C. Boyer, W. Weissflog, G. Pelzl, L.-C. Chien, J. Zasadzinski, J. Watanabe, D. M. Walba, H. Takezoe, and N. A. Clark, *Science* **301**, 1204 (2003).
52. First demonstrated by: D. R. Link, G. Natale, R. Shao, J. E. Maclennan, N. A. Clark, E. Körblova and D. M. Walba, *Science* **278**, 1924 (1997).
53. A. M. Figueireedo Neto and S. R. A. Salinas*The Physics of Lyotropic Liquid Crystals: Phase Transitions and Structural Properties* (Oxford University Press, USA, 2005).
54. N. R. Jana, L. Gearheart, and C. J. Murphy, *Adv. Mater.* **13**, 1389 (2001).
55. N. R. Jana, L. A. Gearheart, S. O. Obare, C. J. Johnson, K. J. Edler, S. Mann, and C. J. Murphy, *J. Mater. Chem.* **12**, 2909 (2002).
56. C. J. Johnson, E. Dujardin, S. A. Davis, C. J. Murphy, and S. Mann, *J. Mater. Chem.* **12**, 1765 (2002).
57. B. D. Busbee, S. O. Obare, and C. J. Murphy, *Adv. Mater.* **15**, 414 (2003).
58. M. Andersson, V. Alfredsson, P. Kjellin, and A. E. C. Palmqvist, *Nano Lett.* **2**, 1403 (2002).
59. Some of these aspects have recently been discussed in a detailed review article. B. L. Cushing, V. L. Kolesnichenko and C. J. O'Connor, *Chem. Rev.* **104**, 3893 (2004).
60. M. C. Daniel and D. Astruc, *Chem. Rev.* **104**, 293 (2004).
61. K. V. Sarathy, G. Raina, R. T. Yadav, G. U. Kulkarni, and C. N. R. Rao, *J. Phys. Chem. B.* **101**, 9876 (1997).
62. H. Choo, E. Cutler, and Y. S. Shon, *Langmuir* **19**, 8555 (2003).
63. W. Wang, S. Efrima, and O. Regev, *Langmuir* **14**, 602 (1998).
64. S. Y. Zhao, S. H. Chen, D. G. Li, X. G. Yang, and H. Y. Ma, *Physica E.* **23**, 92 (2004).
65. S. Chen, H. Yao, and K. Kimura, *Langmuir* **17**, 733 (2001).
66. N. Kanyama, O. Tsutsumi, A. Kanazawa, T. Ikeda, *Chem. Commun.* 2640 (2001).
67. M. Brust, M. Walker, D. Bethell, D. J. Schiffrin and R. J. Whyman, *J. Chem. Soc. Chem. Commun.* 801 (1994).
68. A. Badia, R.B. Lennox, and L. Reven, *Acc. Chem. Res.* **33**, 475 (2000).
69. L. Pasquato, P. Pengo, and P. Scrimin, *J. Mater. Chem.* **14**, 3481 (2004).
70. T. S. Ahmadi, Z. L. Wang, T. C. Green, A. Henglein, and M. A. El-Sayed, *Science* **272**, 1924 (1996).
71. J. M. Petroski, Z. L. Wang, T. C. Green, and M. A. El-Sayed, *J. Phys. Chem. B* **102**, 3316 (1998).
72. J. S. Bradley, B. Tesche, W. Bussner, M. Maase, and M. T. Reetz, *J. Am. Chem. Soc.* **122**, 4631 (2000).
73. (a) N. R. Jana, L. Gearheart, and C. J. Murphy, *Chem. Commun.* 617 (2001); (b) A. Cole and C. J. Murphy, *Chem. Mater.* **16**, 3633 (2004).
74. N. Sertova, M. Toulemonde, and T. Hegmann, *J. Inorg. Organomet. Polym. Mater.* **16**, 91 (2006).
75. R. G. Laughlin, ed., *Cationic Surfactants: Physical Chemistry*, vol 2. (Marcell Dekker Inc., New York and Basel, 1991), pp. 1–40.
76. L. Coppola, R. Gianferri, I. Nicotera, C. Oliviero, and G. A. Ranieri, *Phys. Chem. Chem. Phys.* **6**, 2364 (2004).
77. K. M. McGrath, *Langmuir* 11, 1835 (1995).
78. Z. Liu, Z. Hu, Q. Xie, B. Yang, J. Wu, and Y. Qian, *J. Mater. Chem.* **13**, 159 (2003).
79. B. Gates, Y. D. Yin, and Y. N. Xia, *J. Am. Chem. Soc.* **122**, 12582 (2000).
80. G. S. Attard, J. C. Glyde, and C. G. Göltner, *Nature* **378**, 366 (1995).
81. G. S. Attard, C. G. Göltner, J. M. Corker, S. Henke, and R. H. Templer, *Angew. Chem. Int. Ed.* **109**, 1372 (1997).
82. S. Polarz and M. Antonietti, *Chem. Commun.* 2593 (2002).
83. K. Landskron and G. A. Ozin, *Science* **306**, 1529 (2004).
84. M. Antonietti and G. A. Ozin, *Chem. Eur. J.* **10**, 28 (2004).
85. (a) P. Yang, D. Zhao, B. F. Margolese, B. F. Chmelka and G. D. Stucky, *Chem. Mater.* **11**, 2813 (1999).
86. F. Schüth, *Chem. Mater.* **13**, 3184 (2001).
87. C. T. Kresge, M. E. Leonowicz, W. J. Roth, J. C. Vartuli, and J. S. Beck, *Nature* **359**, 710 (1992).
88. D. Zhao, Q. Huo, J. Feng, B. F. Chmelka, and G. D. Stucky, *J. Am. Chem. Soc.* **120**, 6024 (1998).
89. J. S. Beck, J. C. Vartuli, W. J. Roth, M. E. Leonowicz, C. T. Kresge, K. D. Schmitt, C. T. W. Chu, D. H. Olson, E. W. Sheppard, S. B. McCullen, J. B. Higgins, and J. L Schlenker, *J. Am. Chem. Soc.* **114**, 10834 (1992).
90. J. Y. Ying, C. P. Mehnert and M. S. Wong, Angew. *Chem., Int. Ed.* 38, 56 (1999), and references therein.
91. A. Thomas, H. Schlaad, B. Smarsly and M. Antonietti, *Langmuir* 19, 4455 (2003), and references therein.
92. D. A. Doshi, A. Gibaud, V. Goletto, M. C. Lu, H. Gerung, B. Ocko, S. M. Han, and C. J. Brinker, *J. Am. Chem. Soc.* **125**, 11646 (2003).
93. D. M. Lyons, K. M. Ryan, and M. A. Morris, *J. Mater. Chem.* **12**, 1207 (2002).
94. N. M. Huang, C. S. Kan, and S. Radiman, *Appl. Phys. A* **76**, 555 (2003).
95. Y. Yamauchi, T. Yokoshima, T. Momma, T. Osaka, and K. Kuroda, *J. Mater. Chem.* **14**, 2935 (2004).
96. P. N. Bartlett, P. N. Birkin, M. A. Ghanem, P. Groot, and M. Sawicki, *J. Electrochem. Soc.* **148**, C119 (2001).
97. P. N. Bartlett, B. Gollas, S. Guerin, and J. Marwan, *Phys. Chem. Chem. Phys.* **4**, 3835 (2002).
98. P. A. Nelson, J. M. Elliott, G. S. Attard, and J. R. Owen, *Chem. Mater.* **14**, 524 (2002).
99. P. N. Bartlett and J. Marwan, *Micropor. Mesopor. Mater.* **62**, 73 (2003).
100. I. S. Nandhakumar, J. M. Elliott, and G. S. Attard, *Chem. Mater.* **13**, 3840 (2001).
101. T. Gabriel, I. S. Nandhakumar, and G. S. Attard, *Electrochem. Commun.* **4**, 610 (2002).
102. A. H. Whitehead, J. M. Elliott, J. R. Owen and G. S. Attard, Chem. Commun. 331 (1999).

103. F. Bender, R. K. Mankelow, B. Hibbert, and J. Gooding, *Electroanalysis* **18**, 1558 (2006).
104. J. H. Ding and D. L. Gin, *Chem. Mater.* **12**, 22 (2000).
105. For a review of nanoparticles in micro-phase separated block-copolymers see: A. Haryono and W. H. Binder, *Small* **2**, 600 (2006).
106. T. M. Dellinger and P. V. Braun, *Scripta Mater.* **44**, 1893 (2001).
107. R. Patakfalvi and I. Dékány, *Colloid. Polym. Sci.* **280**, 461 (2002).
108. T. M. Dellinger and P. V. Braun, *Chem. Mater.* **16**, 2201 (2004).
109. G. Zhang, X. Chen, J. Zhao, Y. Chai, W. Zhuang, and L. Wang, *Mater. Lett.* **60**, 2889 (2006).
110. R. C. Smith, W. M. Fischer, and D. L. Gin, *J. Am. Chem. Soc.* **119**, 4092 (1997).
111. G. N. Karanikolos, P. Alexandridis, R. Mallory, A. Petrou, and T. J. Mountziaris, *Nanotechnology* **16**, 3121 (2006).
112. G. N. Karanikolos, N.-L. Law, R. Mallory, A. Petrou, P. Alexandridis, and T. J. Mountziaris, *Nanotechnology* **17**, 2372 (2005).
113. C. J. O'Connor, C. T. Seip, E. E. Carpenter, S. Li, and V. T. John, *Nanostruct. Mater.* **12**, 65 (1999).
114. L. M. Huang, H. T. Wang, Z. B. Wang, A. Mitra, K. N. Bozhilov, and Y. S. Yan, *Adv. Mater.* **14**, 61 (2002).
115. L. Gi, Y. Gao, and J. Ma, *Colloids Surf. A* **157**, 285 (1999).
116. X. Jiang, Y. Xie, J. Lu, L. Zhu, W. He, and Y. Qian, *J. Mater. Chem.* **11**, 1775 (2001).
117. L. Wang, X. Chen, J. Zhao, Z. Sui, W. Zhuang, L. Xu, and C. Yang, *Colloids Surf. A* **257--258**, 231 (2005).
118. X. Jiang, Y. Xie, J. Lu, L. Zhu, W. He, and Y. Qian, *Chem. Mater.* **13**, 1213 (2001).
119. S. Daniels, P. Christian, and P. O'Brien, *J. Exp. Nanosci.* **1**, 97 (2006).
120. M. P. Pileni, B. W. Ninham, T. Gulik-Krzywicki, J. Tanori, I. Lisiecki, and A. Filankembo, *Adv. Mater.* **11**, 1358 (1999).
121. G. D. Rees, R. Evans-Gowing, S. J. Hammond, and B. H. Robinson, *Langmuir* **15**, 1993 (1999).
122. L. Qi, J. Ma, H. Cheng, and Z. Zhao, *J. Phys. Chem. B* **101**, 3460 (1997).
123. J. D. Hopwood and S. Mann, *Chem. Mater.* **8**, 1819 (1997).
124. H. M. Yang, M. Yang, Y. Zhang, and G. X. Chen, *Colloid J.* **66**, 708 (2004).
125. F. Agnoli, W. L. Zhou, and C. O'Connor, *Adv. Mater.* **13**, 1697 (2001).
126. E. E Carpenter, *J. Magn. Magn. Mater.* **225**, 17 (2001).
127. See for example: T. Hegmann, J. Kain, S. Diele, G. Pelzl and C. Tschierske, *Angew. Chem. Int. Ed.* **40**, 887 (2001), and references therein.
128. D. T. McCormick, Z. W. Fordham, and C. A. Guymon, *Liq. Cryst.* **30**, 49 (2003).
129. D. T. McCormick, R. Chavers, and C. A. Guymon, *Macromolecules* **34**, 6929 (2001).
130. C. A. Guymon, L. A. Dougan, P. J. Martens, N. A. Clark, D. M. Walba, and C. N. Bowman, *Chem. Mater.* **10**, 2378 (1998).
131. A. Taubert, *Angew. Chem., Int. Ed.* **43**, 5380 (2004).
132. W. Dobbs, J.-M. Suisse, L. Douce, and R. Welter, *Angew. Chem., Int. Ed.* **45**, 4179 (2006).
133. G. Lattermann, L. Torre Lorente, M. Grudzev, M. Krekhova and N. V. Usoltseva, 21st International Liquid Crystal Conference, Keystone (CO) (Book of Abstracts, 2006). Pp. 218.
134. Y.-G. Kim, S.-K. Oh, and R. M. Crooks, *Chem. Mater.* **16**, 167 (2004).
135. J. H. Fendler and F. C. Meldrum, *Adv. Mater.* **7**, 607 (1995).
136. A. C. Templeton, W. P. Wuelfing, and R. W. Murray, *Acc. Chem. Res.* **33**, 27 (2000).
137. For an example see: N. Perez, M. J. Whitcombe and E. N. Vulfson, *J. Appl. Polym. Sci.* **77**, 1851 (2000).
138. A. Swami, P. R. Selvakannan, R. Pasricha, and M. Sastry, *J. Phys. Chem. B* **108**, 19269 (2004).
139. M. Sastry, in *Colloids and Colloid Assemblies*, F. Caruso, ed.(Wiley-VCH, Weinheim, 2004), pp. 369–397.
140. M. Fukuto, R. K. Heilmann, P. S. Pershan, A. Badia, and R. B. Lennox, *J. Chem. Phys.* **120**, 3446 (2004).
141. M. Ferreira, V. Zucolotto, M. Ferreira, O. N. Oliveira Jr., and K. Wohnrath, *Encyclopedia Nanosci. Nanotechnol.* **4**, 441 (2004).
142. P. Bertoncello, A. Notargiacomo, and C. Nicolini, *Langmuir* **21**, 172 (2005).
143. X. Zhou, C. Liu, Z. Zhang, L. Jiang, and J. Li, *Coll J. Interf. Sci.* **284**, 354 (2005).
144. For a review see: R. Shenhar, T. B. Norsten and V. M. Rotello, *Adv. Mater.* **17**, 657 (2005).
145. R. Elghanian, J. J. Storhoff, R. C. Mucic, R. L. Letsinger, and C. A. Mirkin, *Science* **277**, 1078 (1997).
146. W. Shenton, S. A. Davis, and S. Mann, *Adv. Mater.* **11**, 449 (1999).
147. S. Mann, W. Shenton, M. Li, S. Connolly, and D. Fritzmaurice, *Adv. Mater.* **12**, 147 (2000).
148. C. M. Niemeyer, *Angew. Chem., Int. Ed.* **40**, 4254 (2001).
149. N. L. Rosi, C. S. Thaxton, and C. A. Mirkin, *Angew. Chem., Int. Ed.* **43**, 5500 (2004).
150. N. L. Rosi and C. A. Mirkin, *Chem. Rev.* 105, 1547 (2005), and references therein.
151. S. W. Chung, D. S. Ginger, M. W. Morales, Z. F. Zhang, V. Chandrasekhar, M. A. Ratner, and C. A. Mirkin, *Small* **1**, 64 (2005).
152. For a review see: U. Drechsler, B. Erdogan and V. M. Rotello, *Chem. Eur. J.* **10**, 5570 (2004).
153. Related examples of inorganic lyotropic liquid crystals were summarized in a review paper: A. S. Sonin, *J. Mater. Chem.* **8**, 2557 (1998).
154. A. E. Saunders, A. Ghezelbash, D.-M. Smilgies, M. B. Sigman Jr., and B. A. Korgel, *Nano Lett.* **6**, 2959 (2006).
155. L.-S. Li, J. Walda, L. Manna, and A. P. Alivisatos, *Nano Lett.* **2**, 557 (2002).
156. L.-S. Li and A. P. Alivisatos, *Adv. Mater.* **15**, 408 (2003).
157. L.-S. Li, M. Marjanska, G. H. J. Park, A. Pines, and A. P. Alivisatos, *J. Chem. Phys.* **120**, 1149 (2004).
158. F. Kim, S. Kwan, J. Akana, and P. Yang, *J. Am. Chem. Soc.* **123**, 4360 (2001).
159. C. V. Talapin, E. V. Shevchenko, C. B. Murray, A. Kornowski, S. Forster, and H. Weller, *J. Am. Chem. Soc.* **126**, 12984 (2004).
160. B. A. Korgel and D. Fitzmaurice, *Adv. Mater.* **10**, 661 (1998).
161. M. Li, H. Schnablegger, and S. Mann, *Nature* **402**, 393 (1999).
162. B. Nikoobakht, Z. L. Wang, and M. A. El-Sayed, *J. Phys. Chem. B* **104**, 8635 (2000).
163. T. K. Sau and C. J. Murphy, *Langmuir* **21**, 2923 (2005).
164. N. R. Janan, *Angew. Chem., Int. Ed.* **43**, 1536 (2004).
165. F. Dumestre, B. Chaudret, C. Amiens, M. Respaud, P. Fejes, P. Renaud, and P. Zurcher, *Angew. Chem., Int. Ed.* **42**, 5213 (2003).
166. J. A. C. Veerman and D. Frenkel, *Phys. Rev. A* **45**, 5632 (1992).
167. S. D. Zhang, P. A. Reynolds, and J. S. Dujneveldt, *J. Chem. Phys.* **117**, 9947 (2002).
168. A. B. D. Brown, S. M. Clarke, and A. R. Rennie, *Langmuir* **14**, 3129 (1998).
169. F. M. Kooij and H. N. W. Lekkerkerker, *J. Phys. Chem. B* **102**, 7829 (1998).
170. F. M. Kooij, K. Kassapidou, and H. N. W. Lekkerkerker, *Nature* **406**, 868 (2000).
171. P. Davidson and J.-C. P. Gabriel, *Curr. Opin. Coll. Interf. Sci.* **9**, 377 (2005).
172. J.-C. P. Gabriel, F. Camerel, B. J. Lemaire, H. Desvaux, P. Davidson, and P. Batail, *Nature* **413**, 504 (2001).

173. V. F. Puntes, D. Zanchet, C. K. Erdonmez, and A. P. Alivisatos, *J. Am. Chem. Soc.* **124**, 12874 (2002).
174. M. B. Sigman, A. Ghezelbash, T. Hanrath, A. E. Saunders, F. Lee, and B. A. Korgel, *J. Am. Chem. Soc.* **125**, 16050 (2003).
175. Y.-W. Zhang, X. Sun, R. Si, L.-P. You, and C.-H. Yan, *J. Am. Chem. Soc.* **127**, 3260 (2005).
176. A. Ghezelbash and B. A. Korgel, *Langmuir* **21**, 9451 (2005).
177. K. H. Park, K. Jang, and S. U. Son, *Angew. Chem., Int. Ed.* **45**, 4608 (2006).
178. N. Kanayama, O. Tsutsumi, A. Kanazawa and T. Ikeda *Chem. Commun.* 2640 (2001).
179. I. In, Y.-W. Jun, Y. J. Kim and S. Y. Kim, *Chem. Commun.* 800 (2005).
180. I. Gascon, J. D. Marty, T. Gharsa, and C. Mingotaud, *Chem. Mater.* **17**, 5228 (2005).
181. L. Cseh and G. H. Mehl, *J. Am. Chem. Soc.* **128**, 13376 (2006).
182. L. Cseh and G. H. Mehl, *J. Mater. Chem.* **17**, 311 (2007).
183. M. Büttner, T. Belser, and P. Oelhafen, *J. Phys. Chem. B* **109**, 5464 (2005).
184. M. M. Maye, W. Zheng, F. L. Leibowitz, N. K. Ly, and C. Zhong, *Langmuir* **16**, 490 (2000).
185. Y. Chen, R. E. Palmer, and J. P. Wilcoxon, *Langmuir* **22**, 2851 (2006).
186. K. Kanie and T. Sugimoto, *J. Am. Chem. Soc.* **125**, 10518 (2003).
187. K. Kanie and M. Muramatsu, *J. Am. Chem. Soc.* **127**, 11578 (2005).
188. K. Kanie, S. Hatayama and A. Muramatsu, 21st International Liquid Crystal Conference, Keystone (CO) (Book of Abstracts, 2006), pp. 259.
189. J. Mougous, R. Baker, and D. L. Patrick, *Phys. Rev. Lett.* **84**, 2742 (2000).
190. D. L. Patrick, F. S. Wilkinson, and T. L. Fegurgur, *Proc. SPIE* **5936**, 5936A (2005).
191. C. Lapointe, A. Hultgren, D. M. Silevitch, E. J. Felton, D. H. Reich, and R. L. Leheny, *Science* **303**, 652 (2004).
192. C. Lapointe, N. Cappallo, D. H. Reich, and R. L. Leheny, *J. Appl. Phys.* **97**, 10Q304 (2005).
193. I. Dierking, G. Scalia, P. Morales, and D. LeClere, *Adv. Mater.* **16**, 865 (2004).
194. I. Dierking, G. Scalia, and P. Morales, *J. Appl. Phys.* **97**, 044309 (2005).
195. H. Duran, B. Gazdecki, A. Yamashita, and T. Kyu, *Liq. Cryst.* **32**, 815 (2005).
196. S. Courty, J. Mine, A. R. Tajbakhsh, and E. M. Terentjev, *Europhys. Lett.* **64**, 654 (2003).
197. M. D. Lynch and D. L. Patrick, *Chem. Mater.* **16**, 762 (2004).
198. M. D. Lynch and D. L. Patrick, *Nano Lett.* **2**, 1197 (2002).
199. M. E. Sousa, S. G. Cloutier, K. Q. Jian, B. S. Weissman, R. H. Hurt, and G. P. Crawford, *Appl. Phys. Lett.* **87**, 173115 (2005).
200. G. P. Crawford and R. H. Hurt, in H. S. Nalwa, ed. *Encyclopaedia of Nanoscience and Nanotechnology*, vol 10 (American Scientific Publishers, 2003), pp. 1–27.
201. C. Chan, G. Crawford, Y. Gao, R. Hurt, K. Jian, H. Li, B. Sheldon, M. Sousa, and N Yang, *Carbon* **43**, 2431 (2005).
202. F. R. Hung, O. Guzmán, B. T. Gettelfinger, N. L. Abbott, and J. J. Pablo, *Phys. Rev. E* **74**, 011711 (2006).
203. F. Brochard and P. G. Gennes, *J. de Physique* **31**, 691 (1970).
204. M. Zapotocky, L. Ramos, P. Poulin, T.C. Lubensky, and D. A. Weitz, *Science* **283**, 209 (1999).
205. H. Stark, *Phys. Rep.* **351**, 387 (2001).
206. M. Mitov, C. Portet, C. Bourgerette, E. Snoeck, and M. Verelst, *Nat. Mater.* **1**, 229 (2002).
207. M. Mitov, C. Bourgerette, and F. Guerville, *J. Phys. Condens. Matter* **16**, 1981 (2004).
208. P. Poulin, H. Stark, T. C. Lubensky, and D. A. Weitz, *Science* **275**, 1770 (1997).
209. O. V. Kuksenok, R. W. Rudwandl, S. V. Shiyanovskii, and E. M. Terentjev, *Phys. Rev. E* **54**, 5198 (1996).
210. R. W. Ruhwandl and E. M. Terentjev, *Phys. Rev. E* **56**, 5561 (1997).
211. T. C. Lubensky, D. Pettey, N. Currier, and H. Stark, *Phys. Rev. E* **57**, 610 (1998).
212. H. Stark, *Eur. Phys. J. B* **10**, 311 (1999).
213. H. Stark, J. Stelzer, and R. Bernhard, *Eur. Phys. J. B* **10**, 515 (1999).
214. D. Andrienko, G. Germano, and M. P. Allen, *Phys. Rev. E* **63**, 041701 (2001).
215. B. I. Lev, S. B. Chernyshuk, P. M. Tomchuck, and H. Yokoyama, *Phys. Rev. E* **65**, 021709 (2002).
216. P. Poulin and D. A. Weitz, *Phys. Rev. E* **57**, 626 (1998).
217. O. Mondain-Monval, J. C. Dedieu, T. Gulik-Krzywicki, and P. Poulin, *Eur. Phys. J. B* **12**, 167 (1999).
218. P. Poulin, V. Cabuil, and D. A. Weitz, *Phys. Rev. Lett.* **79**, 4862 (1997).
219. Y. D. Gu and N. L. Abbott, *Phys. Rev. Lett.* **85**, 4719 (2000).
220. J.-C. Loudet, P. Barois, and P. Poulin, *Nature* **407**, 611 (2000).
221. J.-C. Loudet, P. Poulin, and P. Barois, *Europhys. Lett.* **54**, 175 (2001).
222. J.-C. Loudet and P. Poulin, *Phys. Rev. Lett.* **87**, 165503 (2001).
223. J.-C. O. Loudet Mondain-Monval and P. Poulin, *Eur. Phys. J. E* **7**, 205 (2002).
224. P. Poulin and N. O. France's Mondain-Monval, *Phys. Rev. E* **59**, 4384 (1999).
225. J. Fukuda, H. Yokoyama, M. Yoneya, and H. Stark, *Mol. Cryst. Liq. Cryst.* **435**, 723 (2005).
226. H. Stark, *Phys. Rev. E* **66**, 032701 (2002).
227. J. J. Feng and C. Zhou, *J. Colloid Interface Sci.* **269**, 72 (2004).
228. M. Svetec, S. Kralj, and Z. S. Bradač Žumer, *Eur. Phys. J. E* **20**, 71 (2006).
229. P. Kossyrev, M. Ravnik, and S. Žumer, *Phys. Rev. Lett.* **96**, 048301 (2006).
230. P. Tian, G. D. Smith, and M. Glaser, *J. Chem. Phys.* **124**, 161101 (2006).
231. H. Qi and T. Hegmann, *J. Mater. Chem.* **16**, 4197 (2006).
232. O. Guzmán, N. L. Abbott, and J. J. Pablo, *J. Chem. Phys.* **122**, 184711 (2005).
233. H. Qi, A. Lepp, P. A. Heiney, and T. Hegmann, *J. Mater. Chem.* DOI:10.1039/b701411b (2007).
234. V. G. Nazarenko, A. B. Nych, and B. I. Lev, *Phys. Rev. Lett.* **87**, 075504 (2001).
235. I. I. Smalyukh, S. Chernyshuk, B. I. Lev, A. B. Nych, U. Ognysta, V. G. Nazarenko, and O. D. Lavrentovich, *Phys. Rev. Lett.* **93**, 117801 (2004).
236. P. G. Petrov and E. M. Terentjev, *Langmuir* **17**, 2942 (2001).
237. V. J. Anderson, E. M. Terentjev, S. P. Meeker, J. Crain, and W. C. K. Poon, *Euro. Phys. J. E* **4**, 11 (2001).
238. V. J. Anderson, E. M. Terentjev, S. P. Meeker, J. Crain, and W. C. K. Poon, *Euro. Phys. J. E* **4**, 21 (2001).
239. J. Cleaver and W. C. K. Poon, *J. Phys.: Condens. Matter* **16**, S1901 (2004).
240. D. Vollmer, G. Hinze, B. Ullrich, W. C. K. Poon, M. E. Cates, and A. B. Schofield, *Langmuir* **21**, 4921 (2005).
241. W. H. Jeu and R. Eidenschink, *Electron. Lett.* **27**, 1195 (1991).
242. M. Kreuzer, T. Tschudi, and R. Eidenschink, *Mol. Cryst. Liq. Cryst.* **223**, 219 (1992).
243. A. Glushchenko, H. Kresse, V. Reshetnyak, Y. Reznikov, and O. V. Yaroshchuk, *Liq. Cryst.* **23**, 753 (1997).
244. N. J. Diorio Jr., M. R. Fisch, and J. W. West, *Liq. Cryst.* **29**, 589 (2002).
245. M. Boxtel, R. Janssen, D. Broer, H. Wilderbeek, and C. Bastiaansen, *Adv. Mater.* **12**, 753 (2000).

246. M. Boxtel, R. Janssen, C. Bastiaansen, and D. Broer, *J. Appl. Phys.* **89**, 838 (2001).
247. V. Freedericksz and V. Tsvetkov, *Phys. Z. Sov. Union* **6**, 490 (1934).
248. G. Puchkovskaya, Y. Reznikov, A. Yakubov, O. V. Yaroshchuk, and A. Glushchenko, *J. Mol. Struct.* **381**, 133 (1996).
249. S. R. Nersisyan and N. V. Tabiryan, *Appl. Phys. Lett.* **88**, 151106 (2006).
250. L. O. Dolgov and O. V. Yaroshchuk, *Colloid Polym. Sci.* **282**, 1403 (2004).
251. J. Müller, C. Sönnichsen, H. Poschinger, G. Plessen T. A. Klar, and J. Feldmann, *Appl. Phys. Lett.* **81**, 171 (2002).
252. S. Y. Park and D. Stroud, *Phys. Rev. Lett.* **94**, 217401 (2005).
253. P. A. Kossyrev, A. Yin, S. G. Cloutier, D. A. Cardimona, H. Danhong, P. M. Alsing, and J. M. Xu, *Nano Lett.* **5**, 1978 (2005).
254. T. Bezrodna, I. Chashechnikova, L. Dolgov, G. Puchkovska, Ye. Shaydyuk, N. Lebovska, V. Moraru, J. Baran, and H. Ratajczak, *Liq. Cryst.* **32**, 1005 (2005).
255. D. Sikharulidze, *Appl. Phys. Lett.* **86**, 033507 (2005).
256. Y. Williams, K. Chan, J. H. Park, I. C. Khoo, B. Lewis, and T. E. Mallouk, *Proc. SPIE* **5936**, 225 (2005).
257. V. Yu Reshetnyak, S. M. Shelestiuk, and T. J. Sluckin, *Mol. Cryst. Liq. Cryst.* **454**, 201 (2006).
258. S. Sono, T. Miyama, K. Takatoh, and S. Kobayashi, *Proc. SPIE* **6135**, 1 (2006).
259. K. Busch and S. John, *Phys. Rev. Lett.* **83**, 967 (1999).
260. K. Daeseung, J. E. Maclennan, N. A. Clark, A. A. Zakhidov and R. H. Baughman, *Phys. Rev. Lett.* **86**, 4052 (2001), and references therein.
261. A. Jákli, L. S. Almásy Borbély, and L. Rosta, *Eur. Phys. J. B* **10**, 509 (1999).
262. P. Fabre, C. Casagrande, and M. Veyssie, *Phys. Rev. Lett.* **64**, 539 (1990).
263. V. Ponsinet, P. Fabre, M. Veyssie, and L. Auvray, *J. Phys. II* **3**, 1021 (1993).
264. I. Potočová, P. Kopčcansky, M. L. Koneracká Tumčo, J. Jadzin, and G. Czechowski, *J. Magn. Magn. Mater.* **252**, 150 (2002).
265. L. J. Martinez-Miranda, K. McCarthy, L. K. Kurihara, J. J. Harry, and A. Noel, *Appl. Phys. Lett.* **89**, 161917 (2006).
266. E. Matsui and A. Yasuda, *Phys. Rev. E* **56**, 600 (1997).
267. C. S. Pecinovsky, G. D. Nicodemus, and D. L. Gin, *Chem. Mater.* **17**, 4889 (2005).
268. D. W. Bruce, J. W. Goodby, J. R. Sambles, and H. J. Coles, *Phil. Trans. R. Soc. A* **364**, 2567 (2006).